UNIVERSITY OF TARTU
Faculty of Science and Technology
Institute of Technology

Dmytro Fedorenko

The substrate targeting mechanisms of Clb4-Cdk1

Bachelor's Thesis (12 ECTS)

Curriculum Science and Technology

Supervisor(s):
Assoc. Prof., PhD. Ilona Faustova
PhD. Mihkel Örd

Tartu 2022

The substrate targeting mechanisms of Clb4-Cdk1

Abstract:

Cyclin-dependent kinases (CDKs), the master regulators of the cell cycle, phosphorylate hundreds of proteins in an ordered manner to coordinate the sequence of events. In the *S. cerevisiae*, Cdk1 associates sequentially with nine cyclins that direct the kinase to phosphorylate different proteins. Various cyclin docking motifs have been identified on substrates, but very little is known about the substrate targeting mechanisms of G2 cyclin Clb4. Clb4-Cdk1 regulates spindle orientation and has only one known substrate – Kar9. We aimed to study the interactions that mediate phosphorylation of Kar9 by Clb4-Cdk1. We performed sequence analysis of Kar9 and detailed mapping of closely related S phase Clb5 cyclin docking motif NPF on Sic1, which had high similarity to a conserved region in Kar9. Based on this we predicted an NPFF docking motif in Kar9 and identified with *in vitro* kinase assays that NPFF motif is necessary for phosphorylation of Kar9 by Clb4-Cdk1. Also, we found that a phosphorylation site T548 in Kar9 is critical for multiphosphorylation. Thus, multiple interactions that drive the phosphorylation of Kar9 by Clb4-Cdk1 were mapped, providing an insight into the mechanism of substrate recognition of Clb4-Cdk1. Further, we conducted *in silico* analysis to find novel Clb4-Cdk1 targets with the aim to widen the understanding of Cdk1 function in cell cycle regulation.

Keywords: cell cycle, phosphorylation, cyclin-dependent kinase

CERCS: P310 Proteins, enzymology

Clb4-Cdk1 kompleksi substraatide valiku mehhanismid

Lühikokkuvõte:

Rakutsükli kesksed regulaatorid, tsükliinist sõltuvad kinaasid (CDK-d), fosforüleerivad täpse ajastusega sadu valke, et koordineerida rakutsükli protsesse. *S. cerevisiae* Cdk1 seondub järjestikkuselt üheksa tsükliiniga, mis suunavad kinaasi erinevaid valke fosforüleerima. On kirjeldatud mitmeid tsükliinide seondumismotiive substraatvalkudel, aga G2 faasi Clb4-Cdk1 kompleksi substraatide valiku mehhanismidest on väga vähe on teada. Clb4-Cdk1 reguleerib mitootilist käävi ja sel kompleksil on vaid üks teadaolev substraat – Kar9. Käesoleva töö eesmärgiks oli uurida Kar9 fosforüleerimises osalevaid mehhanisme. Me analüüsisime Kar9 valgu järjestust ja kirjeldasime detailselt Sic1 valgus oleva motiivi, mis oli väga sarnane konserveerunud regioonile Kar9 valgus ja mis seondub evolutsiooniliselt lähedase S faasi tsükliiniga Clb5. Sellest lähtuvalt me ennustasime NPFF motiivi Kar9 valgus näitasime *in vitro* kinaasikatsetega, et see motiiv on vajalik Kar9 fosforüleerimiseks Clb4-Cdk1 poolt. Katsete tulemusel selgus, et fosforüleerimissait T548 on vajalik Kar9 multi-fosforüleerimiseks. Seega, me kirjeldasime mitmed interaktsioonid, mis vahendavad Kar9 fosforüleerimist Clb4-Cdk1 poolt, selgitades mehhanisme, mille kaudu Clb4-Cdk1 oma substraate valib. Lisaks viisime läbi *in silico* analüüsi, et leida täiendavaid potentisaalseid Clb4-Cdk1 substraatvalke, laiendamaks meie arusaamist Cdk1 funktsioonidest rakutsükli kontrollimisel.

Võtmesõnad: rakutsükkel, fosforüleerimine, tsükliinist sõltuvad kinaasid

CERCS: P310 Proteiinid, ensümoloogia

TABLE OF CONTENTS

TERMS, ABBREVIATIONS AND NOTATIONS

APC – Anaphase-promoting complex

BSA – Bovine Serum Albumin

CDK – Cyclin-dependent kinase

CSM – Complete Supplement Mixture

DMSO – Dimethyl sulfoxide

EDTA – Ethylenediaminetetraacetic acid

FL – Full-length

HPM – Hydrophobic patch mutant

IPTG – Isopropyl β-D-1-thiogalactopyranoside

$\mathbf{k_{cat}}$ – the catalytic constant, value showing the number of substrate molecules which enzyme site converts to pretuct by unit time, in which enzyme is working with maximal efficiency

$\mathbf{K_M}$ – Michaelis constant, value showing the concentration of the substrate at which the reaction rate is 50% of its maximal value

LB – Lysogeny broth

LP motif – Leucine/Proline-rich G1 cyclin docking motif

OD – Optical density

PBS – Phosphate-buffered saline

PEG – Polyethylene glycol

PMSF – Phenylmethylsulfonyl fluoride

PSSM – Position-specific scoring matrix

SCF – Skp1/Cullin/F-box protein

SDS-PAGE – Sodium dodecyl sulfate–polyacrylamide gel electrophoresis

SPB – Spindle pole body

TAE - Tris-Actetate EDTA

TE – Tris-EDTA

$\mathbf{T_M}$ – Melting temperature

YPD – Yeast Extract–Peptone–Dextrose

INTRODUCTION

Cell cycle is a series of events where the contents of the cell are first duplicated and later segregated between the two daughter cells. The cell cycle events are precisely coordinated via phosphorylation of hundreds of proteins by the cyclin-dependent kinases (CDKs) to ensure error-free cell division. In *Saccharomyces cerevisiae*, cell cycle is driven by one kinase – Cdk1, that sequentially associates with nine cyclins. The temporal control of CDK substrate phosphorylation arises from two mechanisms. First, progression through the cell cycle depends on increasing CDK activity, as initiation of later events requires higher kinase activity. Secondly, different cyclins, which are expressed at different times, direct the kinase complex to phosphorylate distinct substrate proteins.

Cyclins affect the CDK substrate targeting via multiple mechanisms. Cyclins can bind docking motifs in a subset of CDK targets. There are exclusive docking motifs for cyclins from all cell cycle phases, and there are also shared docking motifs that are common for S, G2 and M phase cyclins. Also, different cyclin-CDK complexes localize to different subcellular compartments, thus limiting the pool of substrates that are accessible to the kinase.

While the substrate targeting of most cyclin-Cdk1 complexes in yeast have been characterized in considerable detail, very little is known about the G2 cyclin Clb4. Clb4-Cdk1 is a key regulator of spindle orientation, and it has only one known substrate protein – Kar9. *S. cerevisiae* cyclins are expressed as pairs of paralogs that often have overlapping functions and specificity. However, there seems to be a functional divergence among the G2 phase cyclins. For example, the paralog *CLB3* is unable to rescue the *CLB4* deletion phenotype in spindle orientation. Interestingly, Clb4 has a unique localization among cyclins, as it accumulates distinctly at the microtubule tip, whereas the other cyclins are diffusely in the cytoplasm or nucleoplasm. As deregulation of spindle can lead to errors in chromosome segregation, it is important to understand the regulation mediated by Clb4-Cdk1.

In this thesis, the substrate targeting mechanisms of Clb4-Cdk1 are investigated. For this, we analyse the sequence motifs involved in Kar9 phosphorylation by Clb4-Cdk1. Additionally, we investigate the docking specificity of Clb4-Cdk1 with respect to previously identified cyclin-substrate docking motifs. Finally, we predict novel Clb4-Cdk1 substrate proteins based on colocalization and the presents of NPF motifs. These findings provide insights into Cdk1 regulation and functions in G2 phase.

1 LITERATURE REVIEW

1.1 Overview of the cell cycle

A cell is the smallest unit of life, a building block of every living being on Earth. Cell cycle is a series of events that takes place in a cell to duplicate its material and then divide into two daughter cells. This cycle for cell proliferation consists of four sequential stages: G1, S, G2, and M phases, with distinct events occurring in each phase.

Cyclin-dependent kinase (CDK) is the primary protein responsible for the control of the cell cycle progression, as it sends signals to launch all major cell cycle events. CDK triggers different events by phosphorylating various target proteins, thereby altering their activity, localization, stability or interactions and allowing them to further drive the events of the cell cycle (Morgan, 2007).

CDK itself is activated by activator proteins – cyclins. Different cyclins are expressed in specific cell cycle stages and, in addition to activating CDK, cyclins also guide CDK to phosphorylate specific targets. Altogether, cyclin-CDK complexes drive the phosphorylation of hundreds of key proteins that carry out various cell cycle functions, such as DNA replication and chromosome segregation (Enserink & Kolodner, 2010). *Saccharomyces cerevisiae* has six CDKs, two of which – Cdk1 and Pho85 – are directly involved in cell cycle regulation (Liu & Kipreos, 2000). While Pho85 is non-essential and coordinates cell cycle with metabolism and environmental signals, Cdk1 is essential and sufficient to drive cell cycle progression from G1 to mitosis (Jiménez *et al.*, 2013).

Importantly, the ordering of cell cycle events is directly dependent on CDK activity. For example, if fission yeast cells that are arrested in G1, are released directly to mitotic cyclin-CDK activity, then DNA replication and mitosis occur simultaneously. Dosing CDK activity by adding different concentrations of CDK inhibitor has revealed that cell cycle events from different cell cycle stages have distinct CDK activity thresholds, with later cell cycle events requiring higher CDK activity to be initiated than earlier events (Swaffer *et al.*, 2016).

Cell cycle regulation is essential for proper cell division and therefore the cell's life. Although deregulated cell cycle is a hallmark of cancer, the core network of cell cycle regulation is essential even for the proliferation of cancer cells that divide uncontrollably. The improper behavior of cancer cells is caused by mutations, which mainly prevent apoptosis (pro-

grammed cell death), compromise cell cycle exit, or those that promote S phase entry. Mutations in the mechanisms that prevent mitotic entry and exit, however, are much less frequent. This suggests that some cell cycle regulation mechanisms, such as DNA damage or mitotic checkpoints, are essential for the proper functioning of all cells, even in the endlessly dividing cancer cells (Matthews *et al.*, 2022).

1.1.1 *S. cerevisiae* Cdk1 associates sequentially with nine cyclins

The activity of Cdk1 is mainly controlled by the expression of different cyclins, whose levels vary throughout the cell cycle. *S. cerevisiae* Cdk1 is sequentially activated by nine different cyclins. In G1 phase, Cdk1 is in complex with cyclins Cln1-3, while cyclins Clb5/6 are predominant in the S phase and Clb1-4 are most active in the G2-M phase (Enserink & Kolodner, 2010).

The abundance of cyclins is controlled mainly on the transcriptional level and by cyclin degradation. Progression through the cell cycle is accompanied by waves of the activity of different transcription factors that drive the expression of the proteins that are necessary for the next phases, including the cyclins (Wittenberg & Reed, 2005). The peak Cdk1 activity and cyclin levels are reached in anaphase, where nuclear division occurs. Prior to that point, the anaphase-promoting complex (APC) is launched. In addition to degrading securin to trigger chromosome segregation, APC targets cyclins and sends them to degradation. The degradation of cyclins and suppression of Cdk1 activity is required for cell division and for daughter cells to enter a new cell cycle (Matthews *et al.*, 2022).

In addition to the sequential accumulation of cyclins, they are degraded in a distinct order. For example, the G1 cyclins Cln1/2 are degraded shortly after entry into S phase (Bállega *et al.*, 2019). The degradation of G1 cyclins is controlled by the Skp1/Cullin/F-box protein (SCF) complex that is a key ubiquitin-protein ligase that regulates cyclin levels in addition to APC (Vodermaier, 2004). While the activity of APC is limited to mitosis and G1 phase, SCF is active throughout the cell cycle (Ang & Wade Harper, 2005). Further, S phase cyclins Clb5/6 are degraded at different stages: Clb6 is degraded during the S phase, while Clb5 levels remain high until mitosis, where it gets degraded before anaphase (Jackson *et al.*, 2006). Degradation of APC targets does not occur all at once, it is also ordered. Clb5 is degraded before anaphase among the first APC substrates. This is followed by securin degradation and subsequent separase activation that leads to chromosome segregation and finally degradation of the mitotic cyclins (Lu *et al.*, 2014). Interestingly, G2 phase cyclins

Clb3 and Clb4 follow similar expression profiles in the interphase, but their degradation is different, as Clb4 levels drop rapidly around the time of anaphase entry (14 minutes before the nuclear entry of Whi5-mCherry) similarly to Clb5, whereas Clb3 is stable until late anaphase (**Figure 1**). Such differences in degradation may indicate the need for Clb4 degradation to ensure efficient chromosome segregation, as has been previously found for Clb5 (Faustova *et al.*, 2021). Therefore, while the accumulation of cyclins in interphase is governed by waves of cell-cycle-regulated transcription factors, the temporally resolved degradation of cyclins is controlled by their specificity to different ubiquitin-protein ligases.

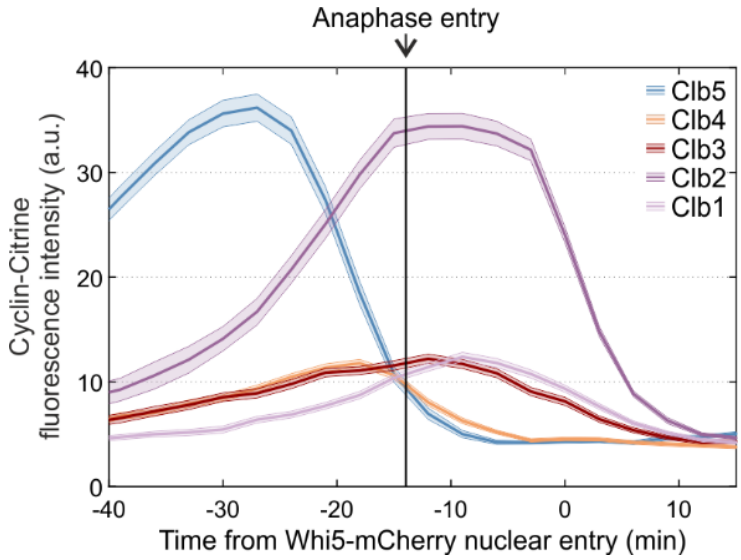

Figure 1. The ordered degradation of cyclins in mitosis. Time-lapse microscopy results showing the fluorescence levels of Citrine-tagged cyclins during mitotic exit. The nuclear entry of Whi5-mCherry, which occurs 14 minutes after entry to anaphase, is used as a reference point in the cell cycle (Faustova *et al.*, 2021).

1.2 Temporal ordering of Cdk1-mediated phosphorylation events

Cdk1 is estimated to phosphorylate over 500 proteins (~10% of the proteome) in a temporally resolved manner (Enserink & Kolodner, 2010; Ubersax *et al.*, 2003). A long-standing question in cell cycle research has been that how does one kinase – Cdk1 – phosphorylate distinct substrates and trigger various events in different cell cycle phases. There are two primary models for the CDK control of the cell cycle: the qualitative and quantitative models. The quantitative model suggests that the ordering of phosphorylation events is achieved due to the increase in CDK activity during the cell cycle, and the phosphorylation of distinct substrates occurs at increasing kinase activity thresholds (later events have higher CDK activity thresholds) (**Figure 2A**) (Swaffer *et al.*, 2016; Uhlmann *et al.*, 2011). On the other

hand, the qualitative model states that the cell cycle is ordered by distinct substrate specificities of successive cyclin abundance waves. In this case, different cyclins target CDK to phosphorylate distinct sets of substrates in different cell cycle phases (**Figure 2B**).

A study has shown that a yeast *S. cerevisiae* strain with all cyclins replaced by copies of mitotic cyclin Clb2, was not able to form buds and, therefore, was not able to replicate and survive. This suggests that this yeast is dependent on G1 cyclin specificity to drive the phosphorylation of some essential proteins involved in morphogenesis. Thus, the quantitative model cannot be fully supported, as cells depend on some cyclin specificity to pass through the cell cycle. The quantitative model, however, provides a robust mechanism for the separation of S and M phases and it could be an ancient mechanism for cell cycle that is driven by one cyclin-CDK complex (Pirincci Ercan *et al.*, 2021). The cyclin specificity could be a way to finetune and maximise temporal resolution of various phosphorylation events (**Figure 2**). Mechanisms that lead to cyclin specificity include directing the kinase to a distinct subcellular compartment, direct binding of the cyclin to specific substrates, and affecting the intrinsic activity of the kinase. Such regulation of CDK activity via cyclins enables the proper order and timing of cell cycle events (Bloom & Cross, 2007).

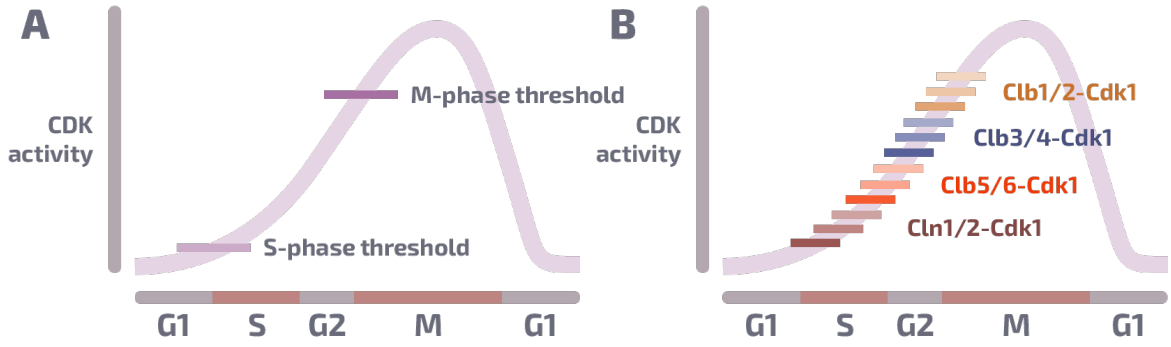

Figure 2. The quantitative and qualitative models of CDK control of the cell cycle. Plots show the oscillation of CDK activity during the cell cycle (thick purple line). (A) According to the quantitative model, the increase in CDK activity leads to phosphorylation of subsequent substrate proteins. Low CDK activity is necessary to trigger S phase and high CDK activity is needed for M phase. (B) According to the qualitative model, the waves of different cyclin-CDK complexes lead to phosphorylation of distinct substrates (Örd, 2021).

1.2.1 Cyclins assign different activation levels to Cdk1

Besides being activators of CDK kinase subunits, different cyclins introduce different activation levels to the CDK. Interestingly, in both yeast and mammals, the rise of intrinsic activity of cyclin–Cdk1 complexes correlates with cyclin's appearance in the cell cycle. Specifically, early cyclins (G1, S) produce kinase complexes with the highest K_M and lowest k_{cat} values towards a peptide with a consensus CDK phosphorylation site, while later complexes (G2, M) have gradually lower the K_M and higher k_{cat} values towards the peptide. These changes in phosphorylation kinetics mean that early cyclin-Cdk1 complexes phosphorylate a substrate peptide with a consensus phosphorylation site, and potentially all Cdk1 substrates that lack specific docking motifs, much slower compared to later complexes. This could be a key mechanism that provides an order to Cdk1-mediated phosphorylation events and that prevents premature phosphorylation of late targets by early cyclin-Cdk1 complexes (Kõivomägi *et al.*, 2011; Örd & Loog, 2019; Topacio *et al.*, 2019).

1.2.2 Cyclin-substrate docking

Cyclins can direct CDK to phosphorylate distinct sets of substrates by recognizing specific amino acid sequences, also known as docking motifs. The cyclin docking motifs are often less than 10 amino acid residues long sequences in intrinsically disordered regions that bind to pockets on the cyclin surface (M. Kumar *et al.*, 2022). Various docking motifs, present in the substrate proteins, increase the phosphorylation of these proteins by recruiting the cyclin-CDK complexes.

Most cyclin-substrate docking interactions take place via a conserved hydrophobic patch on the surface of cyclins (M. Kumar *et al.*, 2022). Some docking motifs are specific to cyclins from a distinct phase, for example, PxxPxF motif that only binds to G2 cyclin Clb3 or LxF that binds M cyclin Clb2. Some other motifs are recognized by a wider range of cyclins, for example, the RxL motif that binds to S, G2 and M cyclins (Örd *et al.*, 2020). All of these three motifs bind to the cyclin hydrophobic patch. Therefore, the hydrophobic patch of closely related cyclins has evolved to recognize distinct motifs but has also retained the ability to bind common motifs, such as RxL. The G1 cyclins Cln1/2 are not known to use the hydrophobic patch for substrate recruitment, instead, they bind LP motifs via a different pocket (Bhaduri *et al.*, 2015). Also, the motifs differ in evolutionary origins, as RxL motifs are important for Cdk1 function in yeasts and human, but some other motifs like PxxPxF and LxF are used only by yeast cyclins (M. Kumar *et al.*, 2022).

Cyclin-substrate docking interactions mediate the cell-cycle-phase-specific phosphorylation of many substrates. Cyclin-substrate docking was initially discovered in G1 and S phase cyclins, leading to a model whereby early CDK complexes compensate for their low intrinsic activity by binding to specific substrates via the docking motifs, enabling efficient phosphorylation of this subset of Cdk1 substrates (Kõivomägi & Skotheim, 2014). Recent studies, however, have shown that cyclin-substrate docking is also critical for G2 and M phase cyclins, thus it is a universal mechanism for Cdk1 substrate targeting throughout the cell cycle (Örd, Venta, *et al.*, 2019). The major cyclin-substrate docking motifs in yeast are shown in **Table 1.**

Table 1. Cyclin-substrate docking motifs. The major docking motifs with description of their functions and corresponding binding pockets in the cyclins.

Motif	***Function***	***Binding pocket***
NLxxxL	Mediates phosphorylation exclusively by Clb5/6-Cdk1 complexes in S phase (Faustova *et al.*, 2021).	Hydrophobic patch
PxxPxF	Directs phosphorylation by Clb3-Cdk1 in the G2 phase (Örd *et al.*, 2020).	Hydrophobic patch
LxF	Governs binding of Clb1/2-Cdk1 in the G2/M phase (Örd, Venta, *et al.*, 2019). Present in both substrate and inhibitor proteins.	Hydrophobic patch
RxL	Mediates binding of Clb1-6-Cdk1 in S, G2, and M phases (Örd, Venta, *et al.*, 2019).	Hydrophobic patch
LP	Drives phosphorylation by Cln1/2-Cdk1 in late G1 phase (Bandyopadhyay *et al.*, 2020).	LP pocket in G1 cyclins
Phosphate binding	Could mediate binding of B-type cyclins in S, G2 and M phases (Asfaha *et al.*, 2022; Yu *et al.*, 2021).	Phospo-binding pocket in B-type cyclins

A structural study of human cyclin B1-Cdk1-separase complex revealed additional cyclin-substrate docking interactions, including a phosphorylation-dependent interaction. During the cell division, in both humans and yeast, segregation of chromosomes is performed by the separase – a large cysteine endopeptidase that cleaves the cohesin subunit Scc1, which is inhibited by securin and Cdk1-cyclin B1 complex (Yu *et al.*, 2021). Human Cdk1-cyclin B1 complex inhibits separase by activating the autoinhibitory loops inside the intrinsically distorted loops of separase, causing it to wrap around the cyclin B1. This loop also interacts with a hydrophobic patch of cyclin B1 through a docking motif which is inverted compared to the RxL motif in other cyclin B1 substrates. Moreover, cyclin B1 was found to contain a phosphate-binding pocket, which contributes to its specificity towards the separase binding (Yu *et al.*, 2021). The phosphate-binding pocket of B-type cyclins is conserved in yeast, where it was found to be important in the phosphorylation of the transcription factor Ndd1 by Clb2-Cdk1 (Asfaha *et al.*, 2022). These findings indicate that there is a vast diversity of interactions between cyclins and substrates but understanding the cyclin specificity and the wider importance of these conserved interactions in cell cycle regulation needs further investigation.

1.2.3 Cyclins direct the localization of Cdk1 complex

In addition to recruiting specific substrates via docking motifs, cyclins can affect substrate targeting of the Cdk1 complex by directing the complex to distinct subcellular compartments. Localization of the Cdk1 complex is driven by the cyclin that has either nuclear import or nuclear export signals (Bloom & Cross, 2007). Differences in the localization can limit the pool of targets available to Cdk1 at different times in the cell cycle. For example, G1 cyclin Cln2 is cytoplasmic, on the other hand, S phase cyclin Clb5 is localized in the nucleus. Importantly, the differences in localization correlate with the functions of these cyclins, as Cln2-Cdk1 regulates bud formation in the cytoplasm and Clb5-Cdk1 triggers DNA replication in the nucleus. Cyclins can also be more precisely localized. For example, mitotic cyclin Clb2 is recruited into the bud neck by Bud3 protein, where it phosphorylates Swe1, leading to degradation of Swe1 (Bailly *et al.*, 2003; Kao *et al.*, 2014; Örd, Venta, *et al.*, 2019).

Compared to other cyclins that are mainly diffused in the cytoplasm or nucleus, the G2 cyclin Clb4 is mainly localized to the microtubule ends that colocalize with the spindle pole bodies (SPBs) (Maekawa & Schiebel, 2004). Clb4-Cdk1 is necessary for proper spindle alignment,

which is an essential step during cell division to guarantee equal segregation of chromosomes. A key step in spindle alignment is governed by Kar9 that selectively localizes to microtubules associated with only one of the SPBs. Kar9 also binds the Clb4-Cdk1 complex, recruiting it to the plus end of astral microtubules. Cdk1-Clb4 in turn regulates the interactions between the microtubule end and subdomains of the bud cortex. It also facilitates the dissociation of the microtubule bud tip and their capture by the bud neck, therefore preventing the preanaphase chromosome spindle from being pulled in the bud (Maekawa & Schiebel, 2004). The distinct localization of Clb4-Cdk1 could limit its substrate pool to SPB and microtubule end proteins. The docking interactions between Clb4 and Kar9 that could mediate the Clb4 localization, however, are not known.

1.2.4 CDK phosphorylation site specificity and Cks1

As discussed above, cell cycle events are ordered by the increase in CDK activity during the cell cycle, – the later an event occurs, the higher the CDK activity threshold for it. This mechanism raises the question of what parameters determine the phosphorylation threshold of a substrate.

Apart from cyclin specificity, there are two other factors that influence the phosphorylation of a substrate by the cyclin-Cdk1 complex: Cdk1 active site specificity and phosphoadaptor protein Cks1 (**Figure 3**).

Cdk1 active site binds and phosphorylates minimal concensus motif S/T-P (where S/T is the phosphorylation site), also referred to as suboptimal phosphorylation site. In case there is a positively charged residue in +3 position from the phosphorylation site (S/T-P-X-R/K sequence), it is considered an optimal or full consensus phosphorylation site (Chi *et al.*, 2008). The difference in phosphorylation rate of a minimal consensus site compared to a full consensus site is in the range of 5-30 times (Örd, Venta, *et al.*, 2019; Suzuki *et al.*, 2015). However, studies have proven that in some cases cyclin-Cdk1 complexes can phosphorylate S/T sites that lack the proline in +1 position. These sites are also named non-S/T-P motifs and their phosphorylation is generally much less efficient and highly dependent on additional docking interactions (Kõivomägi *et al.*, 2013; Örd & Loog, 2019; Suzuki *et al.*, 2015). As the phosphorylation efficiency of different sites varies greatly based on their similarity to the full phosphorylation site consensus, the phosphorylation site specificity could be a major determinant in determining the kinase activity threshold for the given substrate.

The Cdk1 complex contains a third protein, Cks1, that is a phosphoadaptor protein that binds cyclin-Cdk1 complexes and increases their affinity to phosphorylated substrates. This interaction can lead to more efficient phosphorylation of additional sites. Cks1 binds to phosphorylated sites in the substrate, however, it binds only to phospho-threonines (pT-P), but not phospho-serines (**Figure 3**) (Kõivomägi *et al.*, 2013; McGrath *et al.*, 2013). Thus, the distribution of serine- and threonine-based phosphorylation sites in the substrates could affect the kinase activity threshold of the substrate (Kõivomägi *et al.*, 2013).

Many Cdk1 substrates contain multiple phosphorylation sites, some of which can mediate the output of phosphorylation, while others can affect the phosphorylation of other sites by recruiting Cdk1 via Cks1. Interestingly, Cks1-dependent multiphosphorylation is highly distance-dependent, as Cks1 docking only promotes phosphorylation of sites that are at least 12 amino acid residues C-terminal of the Cks1 binding site, and as the distance increases further, the efficiency of phosphorylation decreases (**Figure 3**) (Kõivomägi *et al.*, 2013). Therefore, the relative positions of phosphorylation sites in multiphosphorylation clusters also affects the efficiency of substrate phosphorylation. The more optimally those phosphorylation sites are positioned, the lower the CDK threshold for substrate activation. For example, the presence of a T-P site at least 12 residues N-terminal of the output site increases the phosphorylation of the output site due to Cks1 docking, however, the presence of such site at the distance shorter than 10 amino acid resides will not enhance the multiphosphorylation via Cks1 docking (Kõivomägi *et al.*, 2013; Örd & Loog, 2019).

In conclusion, there are three main factors in the substrates that affect their phosphorylation by cyclin-Cdk1 complexes: Cdk1 phosphorylation sites, cyclin docking sites, and Cks1 phosphoadaptor binding sites (**Figure 3**). Their numbers, proportions, and relative positioning enables Cdk1 to discriminate between hundreds of substrates so that they can be phosphorylated in a timely-resolved manner, ensuring the proper order of cell cycle events (Faustova *et al.*, 2021; Örd, Venta, *et al.*, 2019).

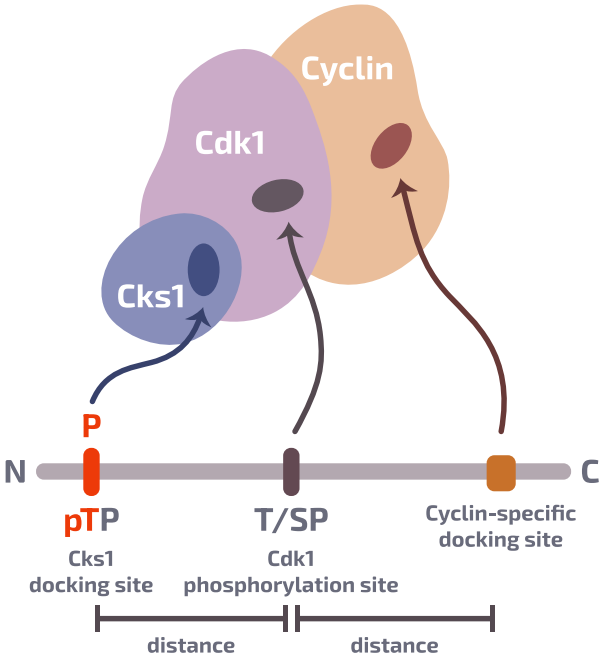

Figure 3. Schematic diagram showing the main interactions between substrate proteins and the CDK complex that determine the phosphorylation rate and specificity. The Cdk1 active site phosphorylates optimal (S/T-P-X-R/K) and suboptimal (S/T-P) sites. Cks1 binds phosphorylated TP sites. Cyclins can interact with substrates via cyclin-specific docking motifs. The effect of the docking interactions on subsequent phosphorylation is dependent on the relative positioning of the docking sites and phosphorylation sites to each other (Örd & Loog, 2019).

1.3 The functions and specificity of G2 cyclin Clb4

While the docking specificities and functions of most yeast cyclins have been characterized in considerable detail, very little is known about G2 cyclin Clb4. The budding yeast cyclins are pairs of paralogs (Cln1/2, Clb5/6, Clb3/4, Clb1/2) that arose from an ancient whole-genome duplication and that have mostly retained similarities in functions and specificity (Enserink & Kolodner, 2010). The functions of G2 cyclins Clb3 and Clb4, however, seem to be diverged, as Clb4-Cdk1 was not able to rescue the loss of Clb3 in PxxPxF-mediated regulation of an SPB protein Csa1 (Örd *et al.*, 2020). Also, loss of Clb4 causes errors in spindle aligment that are not rescued by Clb3 (Maekawa & Schiebel, 2004). This observed divergence and the critical function of Clb4 in spindle alignment, a central cell cycle event, create a need to gain a better understanding of the substrate targeting specificity of Clb4-Cdk1.

1.3.1 Spindle alignment and Kar9

Chromosome segregation is carried out by the pulling forces mediated by mitotic spindle. The spindle organisation is regulated in the cell cycle (**Figure 4**). G1 cells contain one SPB, that is duplicated at G1/S. In G2 phase the duplicated SPBs are separated and spindle forms between the SPBs. The nucleus is pulled into the bud neck by the pulling forces of the astral microtubules. In anaphase the spindle elongates as the two SPBs are pulled to cell poles (Skop *et al.*, 2001).

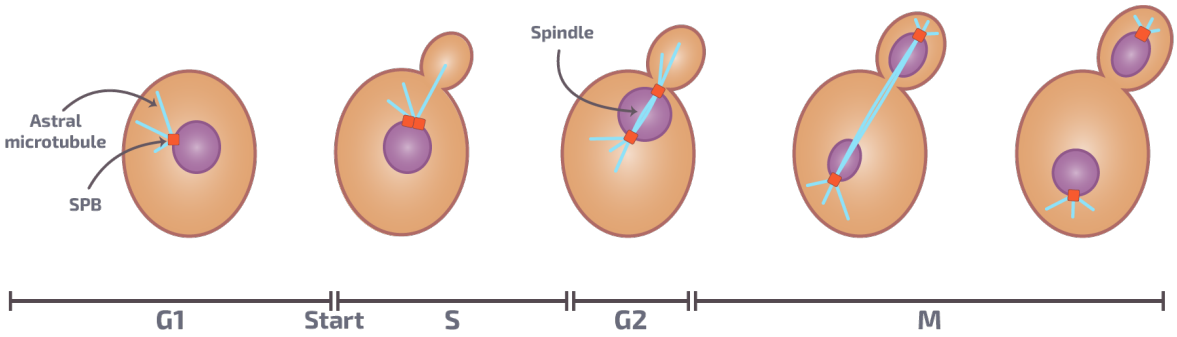

Figure 4. The organisation of the spindle and the SPBs during the cell cycle (Skop *et al.*, 2001)**.**

Kar9 is responsible for the spindle positioning to guide alignment and segregation of chromosomes during cell division in yeast. Kar9 has been found to be targeted by two cyclin-Cdk1 complexes: Clb4- and Clb5-Cdk1 (Bloom & Cross, 2007). While Clb5-Cdk1 also phosphorylates a wide range of replication proteins that have RxL and NLxxxL motifs, Kar9 is the only known substrate for Clb4-Cdk1 (Faustova *et al.*, 2021; Maekawa & Schiebel, 2004).

Kar9 serves as an adaptor for the microtubule tip protein Bim1 and myosin motor Myo2 that displace the astral microtubules along the actin cables (**Figure 5**) (Pietro *et al.*, 2016). The tertiary stucture of Kar9 consists of a folded N-terminal domain in positions 1-400 and an intrinsically disordered C-terminus (positions 401-644) that contains 11 Cdk1 consensus phosphorylation sites and other motifs, such as three Bim1 binding sites, one of which is regulated in cell cycle (Manatschal *et al.*, 2016). Kar9 forms a homodimer with six potential Cdk1 sites surrounding the dimerization interface. The phosphomimetic substitution of these

sites inhibited Kar9 dimerization, displaced Kar9 from microtubules and affected its interaction with the myosin motor Myo2 (**Figure 5**) (A. Kumar *et al.*, 2021). This indicates that the functions of Kar9 are regulated by Cdk1-mediatedphosphorylation.

Asymmetrically dividing cells, such as budding yeast cells, often selectively partition the SPBs between the mother and the daughter cells. In *S. cerevisiae*, the SPB inherited from the previous mitosis goes to the bud, and the new SPB goes to the mother cell. The functions of Kar9 include the asymmetrical selection of old SPB and directing it to the bud (Lengefeld *et al.*, 2017).

Interestingly, it has been observed that phosphorylation by different cyclin-Cdk1 complexes leads to different output functions in Kar9. Clb5-Cdk1 phosphorylation generates Kar9 asymmetry on SPBs, while Clb4-Cdk1 phosphorylation directs the microtubules to the bud cortex (Liakopoulos *et al.*, 2003). Furthermore, distinct phosphorylation sites were identified as the target for each cyclin-Cdk1 complex: Clb5-Cdk1 phosphorylates Kar9 at S496, and Clb4-Cdk1 phosphorylates S197 (Moore & Miller, 2007). Previous studies have only investigated the phosphorylation of full consensus sites S197 and S496, but Kar9 additionally contains 14 minimal consensus phosphorylation sites. Importantly, one of these sites, T625, is part of a Bim1 binding motif, which is regulated during the cell cycle, potentially by phosphorylation (Manatschal *et al.*, 2016). The dynamics and the responsible kinases of phosphorylation of the minimal consensus sites and the mechanism underlying the differences in site specificity of Clb5- and Clb4-Cdk1, however, are not clear.

The overall Kar9 activity during the cell cycle is as follows: 1) Kar9 binds to microtubule ends in the G1 phase; 2) Cdk1 phosphorylates Kar9; 3) Kar9 and Cdk1 move the SPB to the plus end of cytoplasmic microtubules, directed to the bud (A. Kumar *et al.*, 2021; Maekawa *et al.*, 2003).

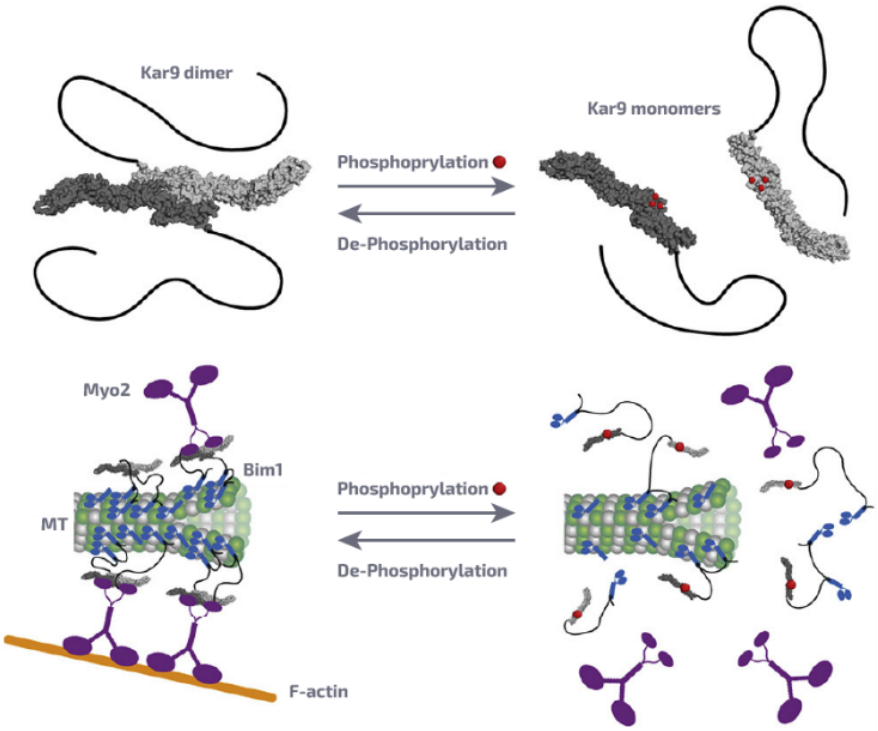

Figure 5. Kar9 conformation and protein-protein interactions are regulated by phosphorylation. Kar9 contains a folded N-terminal domain and an intrinsicailly disordered C-terminal region. In unphosphorylated state Kar9 forms homodimers via the N-terminal domain, but phosphorylated Kar9 is monomeric. The Kar9 C-terminal region binds to Bim1, recruiting it to microtubule ends, where dimeric Kar9 associates with myosin Myo2. Upon phosphorylation, Kar9 is thought to dissociate from the microtubule ends. (A. Kumar *et al.*, 2021).

1.3.2 Kar9 dephosphorylation in anaphase

Cdc14 is a serine/threonine phosphatase that is critical in dephosphorylating Cdk1 targets in late mitosis and G1. It is essential for mitotic exit (Bloom *et al.*, 2011).

Cdc14 is kept inside the nucleolus in an inactive state until anaphase, when it is released into the cytoplasm by two signaling pathways: Cdc14 early anaphase release pathway and mitotic exit network. This division into two phases does not allow the cell to exit mitosis until the spindle is properly positioned, as Cdc14 dephosphorylates multiple proteins involved in spindle positioning during the early anaphase release, and only after that is done, launches the mitotic exit network (Bloom *et al.*, 2011).

Cdc14 dephosphorylates Kar9 in anaphase, which could trigger Kar9 recruitment to both SPBs, as is observed for the CDK phosphorylation site mutant Kar9 (Bloom *et al.*, 2011). This could switch the unidirectional pulling force of the nucleus to the daugther cell into a bidirectional pulling into the opposite side of both mother and daugther cells, which is essential for efficient chromosome segregation (Bloom *et al.*, 2011).

Cdc14 recognizes a PxL docking motif in its key substrates, thereby increasing their dephosphorylation rate, which is necessary for rapid dephosphorylation upon entry to anaphase. The PxL motif is also present in Kar9, where it helps to dephosphorylate Kar9 in anaphase (Kataria *et al.*, 2018). Thus, both phosphatase specificity via the PxL motif and the pre-anaphase degradation of Clb4 (**Figure 1**) could coordinate timely dephosphorylation of Kar9 to ensure efficient chromosome segregation.

While the motifs involved in dephosphorylation of Kar9 are known, the mechansims that mediate Kar9-Clb4 interaction have not been characterised. Errors in chromosome alignment and segregation can lead to aneuploidy, which can lead to cancer (Ben-David & Amon, 2020). Thus, it is critical to understand the mechanisms involved in Clb4-Cdk1-dependent regulation of Kar9 and the spindle positioning. Furthermore, as the same short linear motifs are often present in many proteins, describing these motifs and searching for them in other proteins can provide insights into additional processes. For example, Clb4-Cdk1 is also required for adaptation to glucose starvation and possibly other processes, but the target proteins are not known (Umekawa *et al.*, 2020).

2 THE AIMS OF THE THESIS

Cyclins direct the CDK complex to phosphorylate specific substrate proteins in different cell cycle phases. The discovery of many novel cyclin-substrate docking motifs in the recent years have shown the universal importance of short linear motifs in mediating the CDK substrate targeting. While the substrate targeting mechanisms for most of the *S. cerevisiae* cyclins have been characterized, very little is known about the G2 cyclin Clb4. As Clb4-Cdk1 regulates spindle orientation, a critical process for flawless chromosome segregation and the cell cycle, it is important to understand the substrate targeting of Clb4-Cdk1.

The aims of the thesis are:

- To identify and investigate the sequence motifs in Kar9 that have an impact on its phosphorylation by Clb4-Cdk1.
- To test the importance of the Clb4 hydrophobic patch on Clb4 localization.
- To examine the hydrophobic patch docking specificity of Clb4 using previously characterized docking motifs of different cyclins.
- To predict novel Clb4-Cdk1 substrates.

3 EXPERIMENTAL PART

3.1 MATERIALS AND METHODS

3.1.1 Cloning

We used two approaches for plasmid assembly: insert-vector ligation and full plasmid PCR. For the insert-vector ligation, the desired DNA was first amplified by PCR, during which different mutations or restriction enzyme cutting sites were introduced, followed by purification and restriction digestion of the product. The digested DNA was then ligated into a vector. In case of full plasmid PCR, the PCR primers were designed in a way to amplify the whole plasmid and to introduce the desired mutations. The whole plasmid PCR was purified and ligated, the resulting plasmid DNA was transformed to *Escherichia coli* Turbo cells.

3.1.1.1 PCR

The PCR program and mixture are similar for both and are shown in **Tables 2 and 3**. PCR was performed using Phusion High Fidelity DNA Polymerase (Thermo Fisher Scientific). For insert-vector ligation cloning, the necessary restriction enzyme sites were introduced with the primers.

Table 2. Three-step PCR program. Melting temperature (Tm) was calculated based on the length and composition of primers and extension time was calculated based on the desired product length.

Step	***Temperature***	***Time***	***Number of cycles***
Initial denaturation	98 °C	5 min	1
Denaturation	98 °C	20 s	
Annealing	Tm °C	20 s	30-38
Extension	72 °C	1 kb/30 s	
Final extension	72 °C	5 min	1

Table 3. PCR mixture. PCR mixture for 50 µL final volume.

Reagent	*Volume*
5x Phusion HF buffer	10 µL
F + R primers (10 µM)	1.5+1.5 µL
DNA Template (~5 ng/µl)	1 µL
25 mM dNTPs	0.5 µL
Phusion DNA Polymerase	0.5 µL
MQ H_2O	35 µL

Following the PCR, the obtained mixture was loaded on 1% agarose Tris-Actetate Ethylene-diaminetetraacetic acid (EDTA) (TAE) gel (1% agarose, 40 mM Tris-Acetate pH 8.3, 4 µL/mL Atlas ClearSight DNA stain (BioAtlas), 1 mM EDTA), followed by electrophoresis to verify and isolate the product. The product then was cut out from the agarose gel and purified using FavorPrep™ GEL/PCR Purification Kit (Favorgen), according to the manufacturer's manual.

3.1.1.1.1 Stitching PCR

Some of the insert fragments were assembled with stitching PCR, which enabled to introduce the desired mutations using PCR primers. This method implies the assembly of an insert fragment from two PCR-amplified fragments that are complementary at one end. In this case, the DNA template for the PCR is a mixture of purified PCR fragments that contain regions N- and C-terminal of the introduced mutations. These primary PCR products were added to the PCR mixture (**Table 3**) in 1:1 molar ratio. The program used for the stiching PCR is shown in **Table 4**.

Table 4. Stitching PCR program. Where Tm_1 is calculated based on the annealing region of N and C fragments and Tm_2 is calculated based on the length and compositions of primers. Extension time is calculated based on the desired product length.

Step	*Temperature*	*Time*	*Number of cycles*
Initial denaturation	98 °C	3 min	
Initial annealing	Tm_1 °C	20 s	1
Initial extension	72 °C	3 min	
Denaturation	98 °C	20 s	
Annealing	Tm_2 °C	20 s	30-38
Extension	72 °C	1 kb/30 s	
Final extension	72 °C	5 min	1

Primers were added to the mixture after the first three steps of the PCR reaction.

3.1.1.2 Restriction

After the PCR, electrophoresis and purification of the PCR product, we performed DNA restriction with FastDigest Restriction (ThermoFisher). The vectors used for ligation were also digested using FastDigest restriction enzymes. The restriction mixtures were prepared following the manufacturer's guidelines and are shown in **Tables 5 and 6**.

Table 5. Vector restriction mixture. Restriction mixture for 20 µL final volume.

Reagent	*Amount*
10x FastDigest Green buffer	2 µL
Vector plasmid	1.5 µg
Enzymes	2 µL
FastAP	0.5 µL
MQ H_2O	Up to 20 µL

Table 6. Insert restriction mixture. Restriction mixture for 10 µL final volume.

Reagent	*Volume*
10x FastDigest buffer	1 µL
Insert PCR product	8 µL
Enzymes	1 µL

The restriction mixture was kept at 37°C for 30 min and after that the restricted vector was loaded on 1% agarose TAE gel and the restricted DNA was purified using FavorPrep™ GEL/PCR Purification Kit (Favorgen), according to the manufacturer's manual. The enzymes in the insert mixture restriction were heat-inactivated according to ThermoFisher™'s guidelines. The digested DNA was then used for ligation.

3.1.1.3 Phosphorylation and DpnI treatment of full plasmid PCR products

Following PCR, gel electrophoresis and purification, the full plasmid PCR produts were treated with T4 Polynucleotide kinase (Thermo Fisher) to phosphorylate the DNA ends and with DpnI FastDigest restriction enzyme (Thermo Fisher) to degrade the PCR template DNA. The composition of this reaction mixture is shown in **Table 7**.

Table 7. Full plasmid PCR phosphorylation and DpnI treatment.

Reagent	*Volume*
10x T4 DNA ligase buffer	2 µL
Purified PCR product	8 µL
DpnI FastDigest enzyme	1 µL
T4 Polynucleotide kinase	1 µL
MQ H_2O	6.5 µL

The restriction mixture was kept at 37°C for 30 min. Then, the obtained DNA was used for ligation.

3.1.1.4 Ligation

3.1.1.4.1 Insert-vector ligation

After restriction digestion, we ligated insert DNA and vector DNA in 3:1 molar ratio. The ligation reaction mixture is shown in **Table 8**.

Table 8. Insert-vector ligation. Ligation mixture for 10 µL final volume.

Reagent	*Volume*
10x T4 DNA ligase buffer	1 µL
Insert DNA	3 µL
Vector DNA (~50 ng)	1 µL
T4 DNA ligase	0.5 µL
MQ H_2O	4.5 µL

The ligation was kept for 1-12 hours at 18°C and was then used for bacterial transformation.

3.1.1.4.2 Full plasmid PCR ligation

After the treatment with T4 polynucleotide kinase and DpnI, 1 µL of polyethylene glycol (PEG) 4000 and 0.5 µL of T4 DNA ligase were added to the mixture. The ligation reaction was kept for 10 minutes at room temperature and the ligated DNA was then used for bacterial transformation.

3.1.1.5 Bacterial transformation

To isolate and amplify the ligated plasmids and to verify the correct assembly, they were transformed into competent *E. coli* Turbo (New England Biolabs) cells. The transformation procedure was performed as follows:

1. The competent cells were taken from -80°C freezer and were thawn on ice.
2. 2 µL of ligation mixture was added to 50 µL of competent cell mixture.
3. The mixture was incubated on ice for 30 minutes, follwed by heat-shock at 42°C for 45 s and chilling of cells on ice for 5 minutes.
4. 500 µL of Lysogeny broth (LB) media was added to the transformation mixture.

5. The mixture was incubated at 37°C with constant shaking at 200 rpm for 1 hour.
6. The cells were collected by centrifugation at 6000 rpm for 1 minute.
7. 400 µL of the media was removed and the cells were resuspended in the remaining media.
8. The cells were onto selection plates (LB/agar + 100 µg/mL kanamycin).
9. The plates were incubated overnight at 37°C.

3.1.1.6 Plasmid purification

After transformation, colonies from the plates were put to grow in 4 mL of LB+antibiotic at 37°C, 200 rpm shaking for 6-12 hours. The plasmids were purified using FavorPrep™ Plasmid DNA Extraction Mini Kit (Favorgen), according to the manufacturer's manual.

The obtained plasmids were then sent to Sanger sequencing at the Institute of Genomics Core Facility to verify the correct assembly and sequence. The plasmids constructed in this study are presented in **Table 9**.

Table 9. The plasmids constructed in this study.

Plasmid	*Description*	*Backbone vector*
pMO1028	6xHis-TEV-Kar9(T548A)	pET28a
pMO1029	6xHis-TEV-Kar9(npff)	pET28a
pMO1030	6xHis-Kar9(1-570 AP T548)	pET28a
pMO1031	6xHis-Kar9(1-570 AP)	pET28a
pNPF72	SIC1 (1-90+200-224) F219A	pET28a
pNPF73	SIC1 (1-90+200-224) 222del-AAA	pET28a
pNPF74	SIC1 (1-90+200-224) rvg-AAA	pET28a
pNPF75	SIC1 (1-90+200-224) K216A	pET28a
pNPF76	SIC1 (1-90+200-224) N217A	pET28a
pNPF77	SIC1 (1-90+200-224) P218A	pET28a
pNPF78	SIC1 (1-90+200-224) S221A	pET28a

3.1.2 Protein purification

3.1.2.1 6xHis-Kar9 purification

The correct plasmids were transformed into protein production *E. coli* cells (strain Bl21(DE3)Rosetta). One of the obtained colonies was put to grow in 250 mL volume of LB media at 37°C with 200 rpm shaking until optical density (OD) value of 0.6. Then, the cells were chilled on ice and protein expression was induced with 0.125 mM Isopropyl β-D-1-thiogalactopyranoside (IPTG). The cell culture was placed back to the incubator and grown at 18°C with 200 rpm shaking overnight. After that, the cells were collected by centrifugation at 5500 rpm for 15 minutes, the pellet was washed with 30 mL 1x Phosphate-buffered saline (PBS) and collected by centrifugation again. Finally, the pellet was frozen in liquid nitrogen and placed in -80°C freezer for storage.

We used full-length (FL) Kar9 and Kar9 1-570 proteins for phosphorylation experiments.

3.1.2.1.1 6xHis-Kar9FL purification

Table 10. Buffer compositions. Kar9FL lysis and elution buffer compositions.

Component	***Lysis buffer final concentration***	***Elution buffer final concentration***
NaCl	800 mM	300 mM
Imidazole (pH 8)	10 mM	250 mM
Tris-HCl (pH 7.5)	20 mM	50 mM
Glycerol	10%	10%
β-mercaptoethanol	5 mM	5 mM

The cell pellets were taken from -80°C freezer and left to thaw at room temperature. Next:

1. The cell pellet was resuspended in 7 mL of lysis buffer (**Table 10**) with protease inhibitors (1 mM phenylmethylsulfonyl fluoride (PMSF), 1 µg/mL aprotinin, 1 µg/mL pepstatin A, 1 U/mL DNAse1 and lysozyme (1 mg/mL).
2. Cells were lysed at 4°C for 15 minutes with mixing every three minutes.
3. The mixture was sonicated three times for 20 seconds, and cells were kept on ice for 1 minute between sonications.
4. The lysate was centrifuged at 4°C 14800 rpm for 15 minutes.
5. Next, the Chelating Sepharose columns were prepared by:
    a) Pipetting 100 µL of Chelating Sepharose (GE Healthcare) to the column;
    b) Washing the column with 1 mL of ddH_2O;
    c) Adding 150 µL of 200 mM $NiSO_4$;
    d) Washing the column with 1 mL of lysis buffer.
6. Following centrifugation, the supernatant was transferred to a new tube. The prepared Chelating Sepharose beads were resuspended with the lysate.
7. The mixture was moved to a tube and placed on an end-over-end at 4°C for 30 minutes.
8. The lysate with the beads was transferred to the column, and the lysate was let to flow through.
9. The column was washed four times with 2 mL of lysis buffer, and after that one time with 2 mL of lysis buffer with 20 mM imidazole.
10. The proteins were eluted by adding 4x100 µL of elution buffer (**Table 10**) in a step-wise manner.The second, third and fourth eluates were collected.
11. An aliquot of the protein eluate was pipetted out for determination of protein concentration and purity. The proteins were flashfrozen in liquid nitrogen and stored in -80°C freezer.

3.1.2.1.2 6xHis-Kar9 1-570 purification

Table 11. Buffers used in Kar9 1-570 purification.

Component	*Lysis buffer final concentration*	*Elution buffer final concentration*
NaCl	500 mM	500 mM
Imidazole (pH 8)	-	200 mM
Tris-HCl (pH 7.5)	20 mM	50 mM
Glycerol	10%	10%
β-mercaptoethanol	2 mM	5 mM

The cell pellets were taken out from -80°C freezer and left to thaw at room temperature, after that the following steps were performed.

1. The pellet was resuspended in 10 mL of lysis buffer (**Table 11**) with protease inhibitors (1 mM PMSF, 1 µg/mL aprotinin, 1 µg/mL pepstatin A, 1 U/ml DNAse1) and lysozyme (1 mg/mL).
2. The cells were lysed at 4°C for 10 minutes with mixing the lysate every 2 minutes.
3. The mixture was sonicated three times for 30 seconds, keeping the lysate on ice for 1 minute between the sonications.
4. The lysate was cleared by Centrifugation at 4°C 13000 rpm for 20 minutes.
5. The Chelating Sepharose column was prepared by:
    a) Pipetting 100 µL of Chelating Sepharose to the column;
    b) Washing with 1 mL of ddH_2O;
    c) Adding 100 µL of 200 mM $CoCl_2$;
    d) Washing with 1 mL of lysis buffer.
6. After centrifugation, the supernatant was pipetted to the column, letting it flow through.
7. The column was washed four times with 2 mL of lysis buffer, and after that one time with 1 mL of lysis buffer with 10 mM imidazole.

8. For elution4x100 µL of elution buffer (**Table 11**) was pipetted on the column in four steps and eluates II, III, and IV were collected.
9. An aliquot of the protein eluate was loaded on sodium dodecyl sulfate–polyacrylamide gel electrophoresis (SDS-PAGE) gels to determine concentration and purity. The proteins were frozen in liquid nitrogen and stored at -80°C freezer.

3.1.2.2 Sic1-6xHis purification

The expression plasmids were transformed into protein production *E. coli* cells (strain Bl21(DE3)). One colony was put to grow in 100 mL volume of LB media supplemented with 100 µg/mL kanamycin at 37°C with 200 rpm shaking until OD 0.6. Then, the protein expression was induced with 1 mM IPTG. The cell culture was placed back to the incubator and grown at 37°C with 200 rpm shaking for 3 hours. After that, the cells were collected by centrifugation at 5500 rpm for 15 minutes. Finally, the pellet was frozen in liquid nitrogen and placed in -80°C freezer for storage.

Table 12. Buffers used in Sic1-6xHis protein purification.

Component	***Lysis buffer final concentration***	***Elution buffer final concentration***
Hepes-KOH (pH 7.4)	25 mM	25 mM
NaCl	300 mM	300 mM
Glycerol	10%	10%
Imidazole (pH 8)	-	200 mM

The cell pellets were taken out from -80°C freezer and left to thaw at room temperature, after that the following steps were performed.

1. The pellet was resuspended in 3.5 mL of lysis buffer (**Table 12**) with protease inhibitors (1 mM PMSF, 1 µg/mL aprotinin, 1 µg/mL pepstatin A, 1 U/ml DNAse1) and lysozyme (1 mg/mL).
2. The cells were lysed at 4°C for 15 minutes with mixing the lysate every 3 minutes.
3. The mixture was sonicated three times for 20 seconds, keeping the lysate on ice for 1 minute between the sonications.
4. The lysate was cleared by Centrifugation at 4°C 14800 rpm for 20 minutes.
5. The Chelating Sepharose column was prepared by:
    e) Pipetting 100 µL of Chelating Sepharose (GE Healthcare) to the column;
    f) Washing with 1 mL of ddH_2O;
    g) Adding 150 µL of 200 mM $CoCl_2$;
    h) Washing with 1 mL of lysis buffer.
6. After centrifugation, the supernatant was pipetted to the column, letting it flow through.
7. The column was washed four times with 2 mL of lysis buffer, and after that one time with 1 mL of lysis buffer with 20 mM imidazole.
8. For elution 3x100 µL of elution buffer (**Table 12**) was pipetted on the column in four steps and eluates II and III were collected.
9. An aliquot of the protein eluate was loaded on SDS-PAGE gels to determine concentration and purity. The proteins were frozen in liquid nitrogen and stored at -80°C freezer.

The proteins purified in this study are presented in **Table 13**.

Table 13. The proteins purified in this study.

Plasmid	*Description*	*Backbone vector*
pMO248	6xHis-TEV-Kar9(FL)	pACEMBL
pMO267	6xHis-Kar9(1-570)	pSPCm2
pMO302	6xHis-Kar9(1-570 T548A)	pSPCm2
pMO312	6xHis-Kar9(1-570 S496A)	pSPCm2
pMO459	Sic1(1-33 T2A T5S+3A)-GB1-6xHis	pET28a
pMO460	Sic1(1-26 T2A T5S+3A + PEKLQF)-GB1-6xHis	pET28a
pMO479	6xHis-Kar9(1-570 NPFF-APAA)	pET28a
pMO511	Sic1(1-26 T2A T5S+3A RxL)-GB1-6xHis	pET28a
pMO686	Sic1(1-26 T2A T5S+3A + Fin1KNLLVEL)-GB1-6xHis	pET28a
pMO1028	6xHis-TEV-Kar9(T548A)	pET28a
pMO1029	6xHis-TEV-Kar9(npff)	pET28a
pMO1030	6xHis-Kar9(1-570 AP T548)	pET28a
pMO1031	6xHis-Kar9(1-570 AP)	pET28a
pNPF72	SIC1 (1-90+200-224) F219A	pET28a
pNPF73	SIC1 (1-90+200-224) 222del-AAA	pET28a
pNPF74	SIC1 (1-90+200-224) rvg-AAA	pET28a
pNPF75	SIC1 (1-90+200-224) K216A	pET28a
pNPF76	SIC1 (1-90+200-224) N217A	pET28a
pNPF77	SIC1 (1-90+200-224) P218A	pET28a
pNPF78	SIC1 (1-90+200-224) S221A	pET28a
pKP033	Sic1_PPKGPNFYAK	pET28a
pKP039	Sic1_PRKLQF	pET28a

Plasmids which were not constructed during this study, had been previously made by other members of Mart Loog's lab.

3.1.3 SDS-PAGE

To test the concentration of the purified proteins 2 µL of each protein was loaded on 10% (for Kar9) or 15% (for Sic1-GB1) polyacrylamide gel alongside bovine serum albumin (BSA) (Thermo Fisher) with known concentration for comparison. As a reference, 200, 400, 600, and 800 ng of BSA was loaded on each gel. After the electrophoresis, gels were stained with Coomassie Brilliant Blue R-250 (Applichem) staining solution (40% methanol, 7% acetic acid, 0,025% Coomassie Brilliant Blue R-250), and destained using a high-methanol destaining solution (40% methanol, 7% acetic acid). The destained gels were scanned the Coomassie-stained bands were quantified using ImageQuant TL (Cytiva), and the concentrations of the proteins were calculated based on the calibration curve obtained from the BSA samples.

3.1.4 Kinase assay

3.1.4.1 Kar9

The purified Kar9 proteins were used for *in vitro* kinase assay with phosphor-32 labeling. The reactions were carried out in 20 µL volume. The substrate proteins were diluted to 2 µM concentration in 150 nM NaCl, 25 mM Hepes-KOH (pH 7.4) solution. 5 µL of protein dilution was used for the reaction. The phosphorylation reaction was started by adding 15 µL of enzyme mixture (**Table 14**) to the reaction tube with the substrate protein. The reactions were carried out at room temperature and were terminated after 8 minutes by the addition of 6x SDS sample buffer (60 mM Tris-HCl (pH 6.8), 2% SDS, 10% glycerol, 5% β-mercaptoethanol, 0.01% bromophenol blue), supplemented with 3 mM $MnCl_2$ to the reaction tube.

Then, 10 µL of the reaction mixtures were loaded on 10% SDS-PAGE gels and the remaining volume on 8% polyacrylamide 25 µM Phos-Tag gels. The Phos-tag SDS-PAGE gels were prepared as described in (Örd & Loog, 2020). After the electrophoresis, gels were stained-destained as described in **Section 3.1.2.3**, dried with vacuum pump, and placed in Storage Phosphor Screen cassettes (GE Healthcare) for 1-3 days to collect the ^{32}P signal.

The Storage Phosphor Screen was scanned on an Amersham Typhoon^{TM} laser scanner. The obtained signals were quantified with ImageQuant TL.

Table 14. Enzyme mixture for kinase assay with Kar9 and Clb4-Cdk1. Enzyme mixture composition for 1 reaction (15 µL/reaction).

Component	*Volume*
5x Kinase buffer (Table 15)	4 µL
Insulin (Sigma-Aldrich, 9.5-11.5 mg/mL)	0.4 µL
Cks1 (40 µM)	0.25 µL
Clb4-Cdk1 (100 nM)	0.05 µL
ATP* (PerkinElmer, 10 mCi/mL)	0.1 µL
MQ H_2O	10.4 µL

Table 15. 5x Kinase buffer. 5x Kinase buffer composition.

Component	*Final concentration*
Hepes-KOH (pH 7.4)	12.5 µM
NaCl	25 µM
$MgCl_2$	1.25 µM
ATP	0.125 µM

3.1.4.2 Sic1 kinase assays

The purified Sic1 proteins were used for *in vitro* kinase assay with phosphor-32 labeling. The reactions were carried out in 20 µL volume. The substrate proteins were diluted to 4 µM concentration in elution buffer (**Table 12**). 10 µL of protein dilution was used for the reaction. The phosphorylation reaction was started by adding 10 µL of enzyme mixture (**Table 16**) to the reaction tube with the substrate protein. The reactions were carried out at room temperature and were terminated after 4 and 8 minutes by pipetting the 8 µL of the reaction mixture to the tube containing 9 µL of 2x SDS sample buffer (20 mM Tris-HCl (pH 6.8), 0.66% SDS, 3.33% glycerol, 1.66% β-mercaptoethanol, 0.0033% bromophenol blue).

Then, the reaction mixtures were loaded on 15% acrylamide SDS-PAGE gels. After the electrophoresis, gels were stained-destained as described in **Section 3.1.2.3**, dried with vacuum pump, and placed in Storage Phosphor Screen cassettes (GE Healthcare) for 1-3 days to collect the ^{32}P signal.

The Storage Phosphor Screen was scanned on an Amersham Typhoon™ laser scanner.

Table 16. Enzyme mixture for kinase assay with Sic1. Enzyme mixture composition for 1 reaction (10 µL/reaction).

Component	***Volume***
5x Kinase buffer (Table 15)	4 µL
BSA (ThermoFisher, 20 mg/mL)	0.2 µL
Cks1 (40 µM)	0.25 µL
Clb3/4/5-Cdk1 (100 nM)	0.05 µL
ATP* (PerkinElmer, 10 mCi/mL)	0.1 µL
MQ H_2O	5.6 µL

3.1.5 Yeast transformation

PCR and homologous recombination based approach was used to tag Clb4 with Citrine. For this, Citrine coding sequence together with natNT2 antibiotic resistance gene was PCR-amplified with primers that had homologous regions to the C-terminal region of *CLB4*, as described previously (Janke *et al.*, 2004). The PCR product was purified and transformed into MÖ114 (*W303 MATa bar1Δ::hisG spc42::SPC42-mCherry::kanMX*) and MÖ402 (*W303 MATa bar1Δ::hisG spc42::SPC42-mCherry::kanMX clb4::clb4(hpm)*) *S. cerevisiae* yeast strains. The transformation procedure went as follows:

1. The yeast strain was grown in 25 mL of Yeast Extract–Peptone–Dextrose (YPD) media at 30°C, 160 rpm shaking, until OD of 0.4-0.8.
2. The cells were collected by centrifugation at 3100 rpm for 1 minute.
3. The pellet was resuspended in 1 mL PL1 buffer (100 mM lithium acetate in 0.5x Tris-EDTA (TE) buffer)
4. The cells were centrifuged at 3200 rpm for 1 minute.

5. The buffer was removed, and the cells were resuspended in two times the cell volume of PL1 buffer.
6. The mixture was incubated at room temperature for 10 minutes.
7. At the same time, Salmon Sperm DNA solution (5 mg/mL) was heated at 100°C for 10 minutes to ensure it is single-stranded.
8. 40 µL of the purified PCR product was mixed with 10 µL of the Salmon Sperm DNA solution, followed by addition of 100 µL of the cell suspension.
9. 700 µL of PL2 buffer (40% PEG 3350, 100 mM lithium acetate, 10 mM Tris-HCl (pH 8), 1 mM EDTA) and 48 µL of Dimethyl sulfoxide (DMSO) were added to the transformation mixture, followed by thorough mixing.
10. The transformation mixture was incubated at 42°C for 40 minutes, followed by chilling the cells on ice for 2 minutes.
11. The mixture was centrifuged at 6000 rpm for 30 seconds.
12. The buffer was removed, and the cells were resuspended in 1 mL of 1xTE buffer.
13. The mixture was centrifuged at 3200 rpm for 1 minute.
14. The buffer was removed, and the cells were resuspended in 100 µL of 1xTE buffer.
15. The cells were plated onto YPD plates and grown at 30°C incubator overnight. The cells were then replica-plated onto YPD+clonNAT (Jena Bioscience, 100 µg/mL) selection plates.
16. The plates were incubated for 2-3 days at 30°C.

3.1.6 Time-lapse fluorescence microscopy

After the yeast transformation, colonies from the plates were put to grow in 3 mL of Complete Supplement Mixture (CSM) media with 2% glucose (20 g/L glucose (Oriola), 0.79 g/L CSM powder (Formedium), 7 g/L yeast nitrogen base without amino acids (BD Biosciences) at 30°C with 160 rpm shaking for 3-6 hours until OD 0.6.

Then 0.2 µL of the cell mixture was pipetted onto a 0.08 mm micro cover glass and covered with a small 1 mm thick piece of 2% NuSieve GTG agarose (Lonza) with CSM and 2% glucose. The agar medium pieces were covered with a smaller cover glass to keep the agarose pieces from drying, and this construction was further covered with a plastic cover to prevent evaporation.

Obtained assembly was put into the Zeiss Axio Observer.Z1 microscope with 63x/1.4 Oil M27 Plan-Apochromat objective (Zeiss), DefiniteFocus, Colibri LED module and Temp-Control 37-2 (Pecon). Microscopy experiment lasted 8 hours with 3 minute intervals between the images. Images were taken in three channels: Phase contrast, Citrine and mCherry. Images of the Citrine channel were taken using 505 nm LED-Module with 46 HE reflector (Zeiss), and 500 ms exposure time; mCherry channel used 540-580 nm LED-Module with 61 HE reflector (Zeiss), and 750 ms exposure time.

Obtained images were processed using Matlab, with use of custom-made segmentation and quantification programs (Doncic *et al.*, 2013; Örd, Möll, *et al.*, 2019). Segmentation of the cells was performed on phase contrast images, followed by quantification of the signal in fluorescence channels. Clb4-Citrine SPB localization was quantified as colocalization of Citrine signal with Spc42-mCherry signal. In the final step of the analysis, cells were synchronized at the anaphase timepoint that was determined visually based on Spc42-mCherry. Clb4-Citrine data in the range from -45 min to +45 minutes from anaphase onset was collected. Finally, the average of Citrine fluorescence levels at the SPBs from all analyzed cells were plotted with ±SEM errorbars.

3.1.7 Sequence alignment and PSSM analysis

For conservational analysis of Kar9 and Kar1, first the sequences of Kar9 and Kar1 homologs from yeasts were obtained using Basic Local Alignment Search Tool (BLAST) (https://blast.ncbi.nlm.nih.gov/Blast.cgi) using *S. cerevisiae* Kar9 and Kar1 protein sequences as the query. These sequences were then aligned using ClustalW in BioEdit (Thompson *et al.*, 1994).

PSSMSearch was used for prediction of NPF motifs (Krystkowiak *et al.*, 2018). The NPF-containing peptides from Sic1 and Kar9 were aligned and used as input for PSSMSearch, where the motifs were searched from the intrinsically disordered regions (IUPred score > 0.5) of *S. cerevisiae* proteome. Further, NPF was set as the motif consensus.

3.2 RESULTS AND DISCUSSION

3.2.1 NPFF is a Clb4/5 docking motif

Kar9 contains a folded domain in the N terminus and an intrinsically disordered C terminus (**Figure 5**) (A. Kumar *et al.*, 2021). The Cks1-Cdk1-cyclin complex is known to bind various motifs that are in the intrinsically disordered regions. At the beginning of the project, we analyzed the alignment of Kar9 protein sequences from different yeasts with the aim to find conserved regions (**Figure 6**). While most of the intrinsically disordered C terminus of Kar9 is very variable within the alignment, a number of conserved motifs could be observed. From this sequence alignment we identified a conserved sequence ^{489}NPFF^{492} that is around 15 amino acid residues N-terminal of the Cdc14 docking motif PxL (Kataria *et al.*, 2018). Side-by-side cyclin and Cdc14 phosphatase docking motifs have been found in other Cdk1 targets, which promted us to investigate whether the conserved NPFF sequence is a docking motif for Clb4.

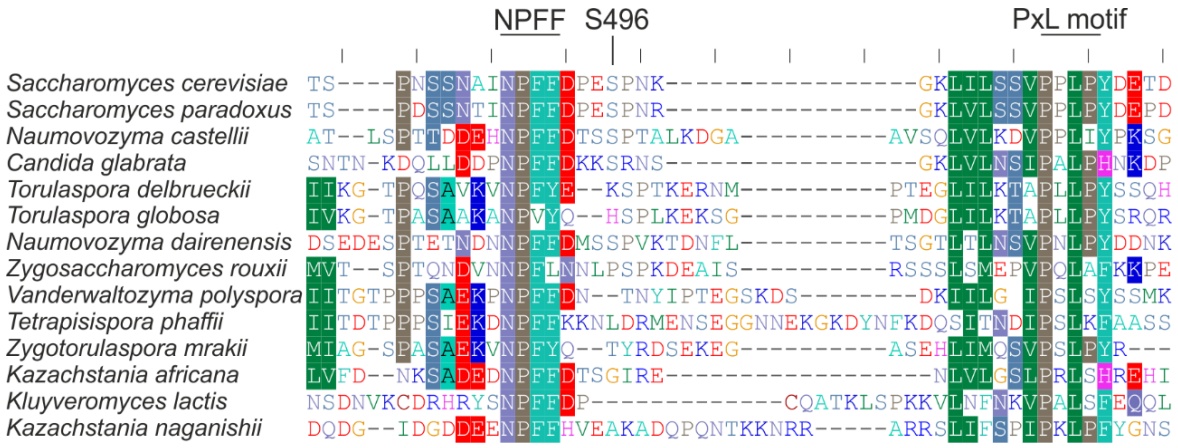

Figure 6. The intrinsically disordered Kar9 C terminus contains a conserved NPFF sequence and a PxL motif. Multiple sequence alignment of Kar9 homologs present in different species of yeast. The Kar9 region from positions 480-516 is shown. The conserved amino acid sequences are shown with color filling.

Previous studies have found that a similar NPF sequence was also present in Sic1, where it mediates phosphorylation by Clb5-Cdk1, but the docking of Clb4-Cdk1 to that motif has not been tested (Schilf, 2018). To gain a better understanding of the NPF motif, we conducted an *in vitro* kinase assay with Clb5-Cdk1 to test the impact of single or multiple residue mutations of amino acids within and around the NPF motif in Sic1 (**Figure 7**).

The assay revealed that disruption of each residue in the NPF sequence reduced the phosphorylation of Sic1 by Clb5-Cdk1 up to 10 times compared to the wild-type Sic1 protein (**Figure 7**). Mutations to the residues surrounding the NPF sequence (213RVG, K216, S221 and 222DEL) had minor effect of the phosphorylation by Clb5-Cdk1 (**Figure 7**). This supports the hypothesis that NPF sequence forms the core of a docking motif for Clb5-Cdk1.

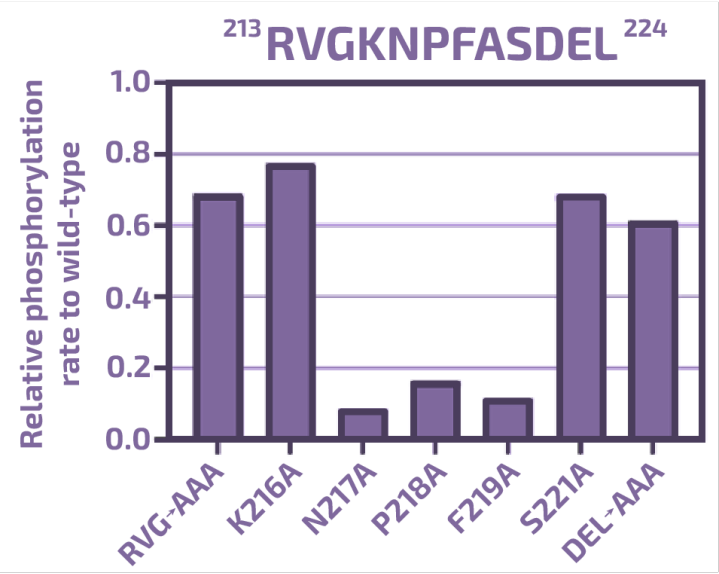

Figure 7. Mapping of the NPF docking motif of Clb5-Cdk1 in Sic1. Kinase assay results showing the relative phosphorylation rates of the indicated Sic1 mutant proteins compared to the wild-type Sic1 version by Clb5-Cdk1.

Next, we tested the effect of mutating the ^{489}NPFF^{492} motif in Kar9 on its phosphorylation by Clb4-Cdk1 in an *in vitro* phosphorylation assay. To gain a deeper inight into Kar9 phosphorylation, the reactions were separated using Phos-tag SDS-PAGE that in addition to molecular weight resolves proteins based on the number of phosphates attached. While wild-type Kar9 was multiphosphorylated by Clb4-Cdk1, almost complete loss of Kar9(1-570) phosphorylation was observed when the NPFF motif was mutated to alanines (**Figure 8A, B**). This indicates that the NPF motif in Sic1 and NPFF in Kar9 are functional docking motifs for Clb5- and Clb4-Cdk1 complexes. Compared to the NPF motif mapping in Sic1 (**Figure 7**), the Kar9 sequence alignment also indicates the functional relevance of F492 and D493 that follow the 489NPF (**Figure 6**), but more detailed experimental mapping is required to identify the determinants of the Clb4 binding motif in Kar9 and to understand whether there are differences in the cyclin specificity of the two NPF motifs.

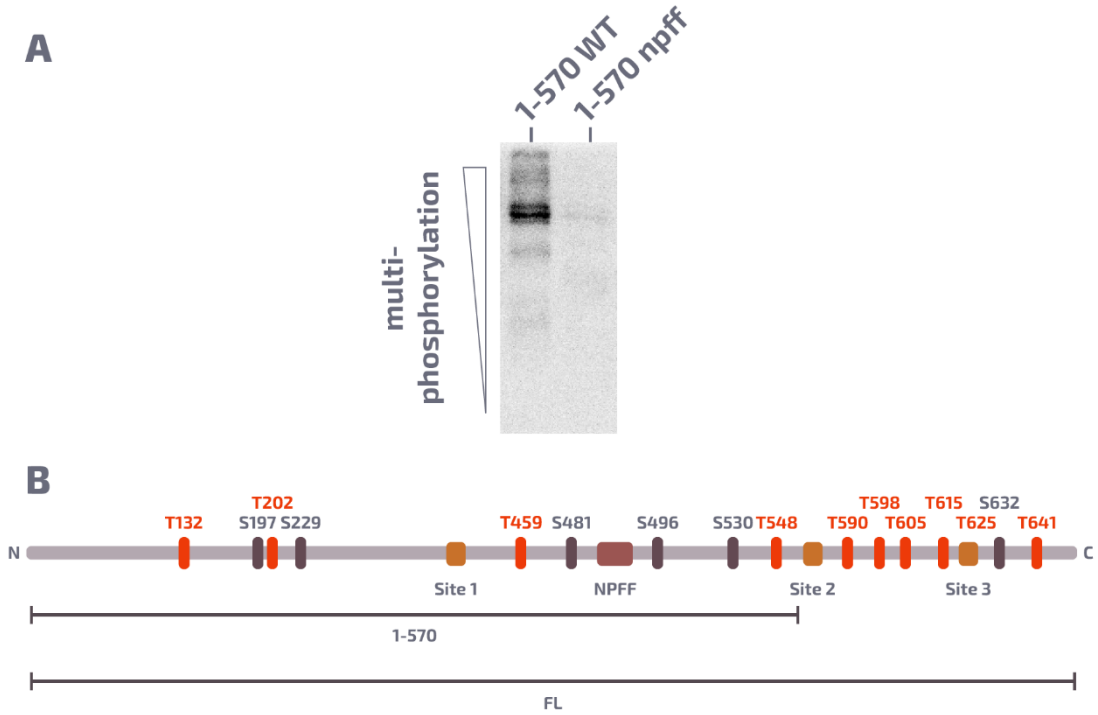

Figure 8. NPFF motif in Kar9 is essential for phosphorylation by Clb4-Cdk1. (A) Phosphorylation reactions of Kar9 and Clb4-Cdk1 were resolved by Phos-tag SDS-PAGE. An autoradiograph showing the phosphorylation of Kar9 by Clb4-Cdk1 is shown. (B) Schematic of Kar9 protein with the docking sites depicted according to their positioning in the protein.

3.2.2 Multiple docking interactions drive multiphosphorylation of Kar9

While previous studies have only investigated the phosphorylation of S197 and S496, which are the only full consensus CDK sites in Kar9, however, Kar9 also contains 14 minimal consensus sites (**Figure 8B**) and analysis of the kinase assay with Clb4-Cdk1 using Phos-tag SDS-PAGE revealed phosphorylation of multiple sites (**Figure 8A**). This prompted us to investigate the multisite phosphorylation in more detail. As it is difficult to resolve large proteins with a large number of phosphates with Phos-tag SDS-PAGE, we used a truncated form of Kar9 containing positions 1-570. This truncation removes seven CDK consensus sites from the C terminus, but retains the NPFF motif.

We tested the effect of different Kar9 phosphorylation site mutations on its phosphorylation by Clb4-Cdk1 *in vitro*. To better observe the impact on total phosphorylation, we analysed the phosphorylation reactions with conventional SDS-PAGE. This revealed that in Kar9(1-570), mutation of the full consensus site S496 to alanine decreased Kar9 phosphorylation by almost two-fold (**Figure 9A**). Interestingly, a similar decrease was observed when a minimal consensus site T548 was mutated (**Figure 9A**). Mutation of all CDK consensus sites in the

disordered C terminus (Kar9 AP, mutations S481A, S496A, S530A, T548A) caused almost complete loss of phosphorylation by Clb4-Cdk1 (**Figure 9A**), although this protein still contains the full consensus site S197. S197 is located in the folded domain and its phosphorylation is important for Kar9 regulation *in vivo* (Maekawa *et al.*, 2003). This assay indicates that S197 could be phosphorylated at very low efficiency compared to the C-terminal sites, which could be due to lower accessibility of S197. High local concentration of Kar9 and Clb4-Cdk1 *in vivo*, driven by co-localization at the microtubule ends could be necessary for phosphorylation of S197. Alternatively, additional proteins that are on the microtubule tip might be necessary to enable S197 phosphorylation. Clb4-Cdk1 and Kar9 interact with several other proteins at the microtubule end, which could affect the phosphorylation of Kar9 (A. Kumar *et al.*, 2021). Kar9(1-570) mutant where all C-terminal sites except for T548 are mutated to alanine was phosphorylated with similar rate as the S496A mutant. These results indicate that S496 and T548 are the main phosphorylation sites in Kar9(1-570).

For analysis of multisite phosphorylation, the same reactions were separated with Phos-tag SDS-PAGE. Interestingly, mutation of S496 had a very minor effect on the multiphosphorylation pattern (**Figure 9B**). However, when T548 was mutated, complete loss of multiphosphorylation was observed. The residues that flank a phosphorylation site can affect how phosphorylation at that site is resolved during Phos-tag SDS-PAGE (Örd & Loog, 2020). This seems to apparent with S496 and T548 as well, as the phospho-protein containing only T548 (AP T548) runs higher in the gel than the T548A mutant (**Figure 9B**). Based on this, we propose that the lowest band corresponds to phosphorylated S496 (observed in T548A mutant), and the second band is singly phosphorylated T548 (observed in WT, S496A and AP T548). The higher bands are presumably multiphosphorylated products. This analysis suggests that T548 promotes multisite phosphorylation of Kar9, as the multiphosphorylation was significantly decreased in the T548A mutant compared to the wild-type (**Figure 9B**). This also holds true for full-length Kar9 mutants, as the T548A mutant runs lower in Phos-Tag SDS-PAGE comparing to wild-type (**Figure 9C**), indicating loss of multiphosphorylation. The npff mutant was much less phosphorylated compared to wild-type, showing that the NPFF motif is essential for the phosphorylation of the full-length Kar9 as well (**Figure 9C**).

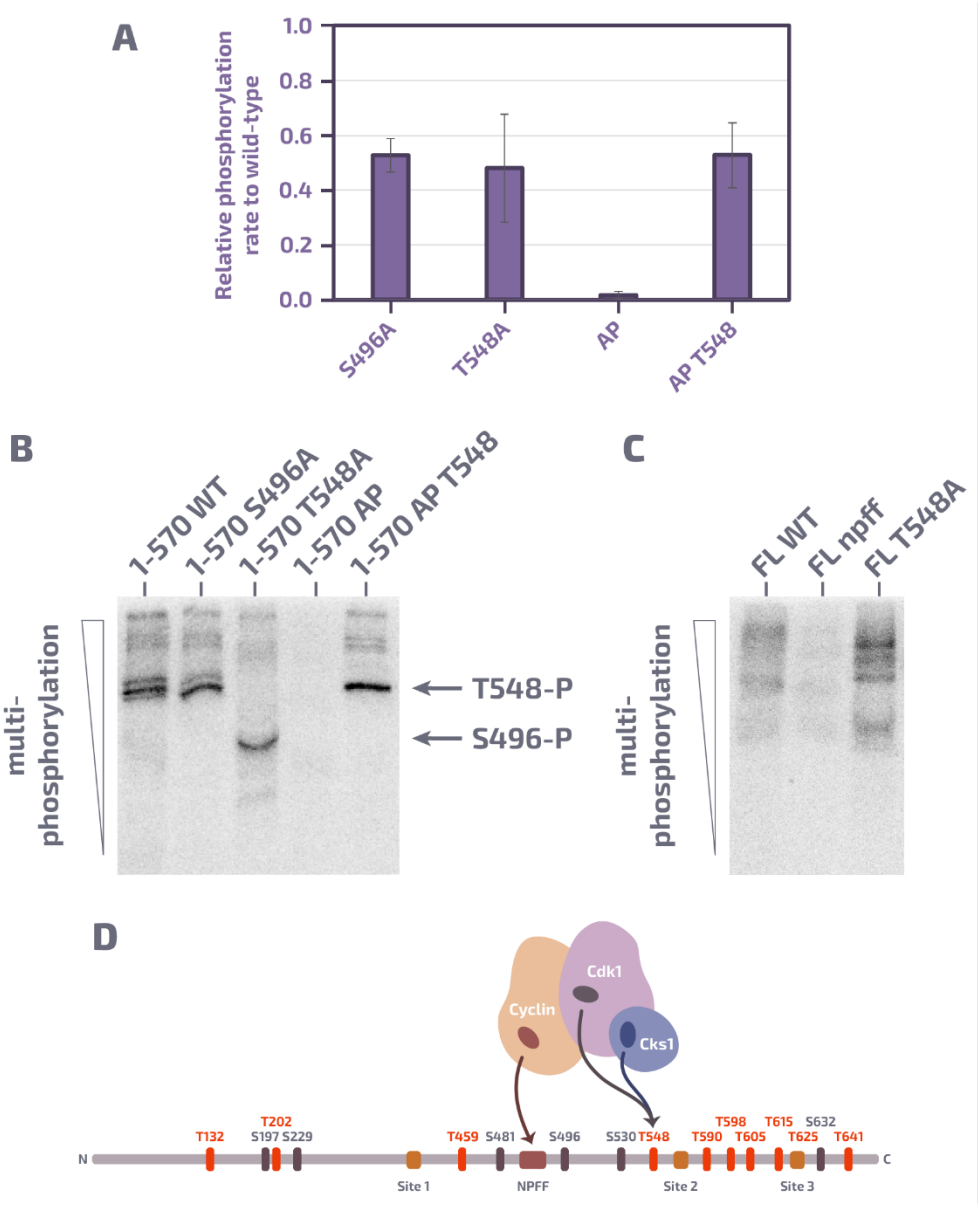

Figure 9. S496 and T548 are the main phosphorylation sites in Kar9(1-570). (A) Plot showing the relative phosphorylation rate of the indicated Kar9 1-570 mutant compared to the wild-type. The values are average from two experiments with standard deviation error bars.(B, C) Autoradiographs showing multisite phosphorylation of the indicated mutants of Kar9 1-570 (panel B) and FL (panel C) by Clb4-Cdk1. The phosphorylation reactions were separated by SDS-PAGE. (D) Schematic of a possible sequence of phosphorylation events driving multiphosphorylation of Kar9 by Clb4-Cdk1.

Phosphorylated TP sites are known to drive multiphosphorylation via Cks1 docking, however, Cks1 binding sites must be N-terminal of the secondary sites (Kõivomägi *et al.*, 2013). As T548 is the most C-terminal site in Kar9(1-570), its effect cannot be mediated by Cks1. Recently, a conserved phosphate-binding pocket of B-type cyclins cyclin binding to

phosphorylated sites has been characterized (Asfaha *et al.*, 2022; Yu *et al.*, 2021). While the sequence determinants of the phosphorylation-dependent cyclin binding sites are not known, there is preliminary evidence that mutation of the phosphate-binding pocket in Clb4 decreases Kar9 multiphosphorylation by Clb4-Cdk1 similarly as mutation of T548 (unpublished results). From the aforementioned results (**Figure 8A, 9**), we propose the possible progression of the Kar9 phosphorylation by Clb4-Cdk1: Clb4 binds the NPFF motif in Kar9 and phosphorylates T548, which, in turn, allows further phosphorylation of other sites, thus enabling multisite phosphorylation (**Figure 9D**). This is supported by the absence of singly phosphorylated S496 band in Kar9 WT reactions (**Figure 9B**). Poor primary phosphorylation of S496 could be due to S496 being only four amino acid residues away from the NPFF (**Figure 6**), as previous studies of cyclin docking motifs have found that the motif and phosphorylation site need to bind simultaneously and for this, a longer minimal distance between the two elements is required (Kõivomägi *et al.*, 2013; Takeda *et al.*, 2001).

3.2.3 The cyclin hydrophobic patch is necessary for Clb4 localization

Clb4 localizes on the microtubule tips by interacting with Kar9 (Maekawa & Schiebel, 2004). Most cyclin-substrate interactions are mediated by the cyclin hydrophobic patch (M. Kumar *et al.*, 2022). We mutated the hydrophobic patch (HPM) in Clb4 and conducted time-lapse fluorescence microscopy to study its effect on Clb4 localization (**Figure 10**). The microtubule ends co-localize with SPBs. For this reason, we studied the co-localization of Clb4-Citrine and Spc42-mCherry, which is a marker for SPBs.

In the microscopy experiments, wild-type Clb4-Citrine was observed as a distinct dot that co-localized with Spc42-mCherry (**Figure 10A**). This is in correlation with previously published results (Maekawa & Schiebel, 2004). Clb4(hpm)-Citrine, however, was dispersed in the nucleus with no clear accumulation at the SPBs (**Figure 10B**). Quantification of the Clb4-Citrine signal that is colocalized with Spc42-mCherry revealed a gradual accumulation of Clb4 in the region of SPBs, on the microtubule ends during the cell cycle, peaking at the onset of anaphase, after which Clb4 is rapidly degraded (**Figure 10C**). Compared the wild-type, the accumulation of Clb4(hpm)-Citrine signal overlapping with the SPBs was lower and could reflect the diffuse nuclear signal, that overlays the SPBs. This analysis shows that the hydrophobic patch is necessary for proper Clb4 localization.

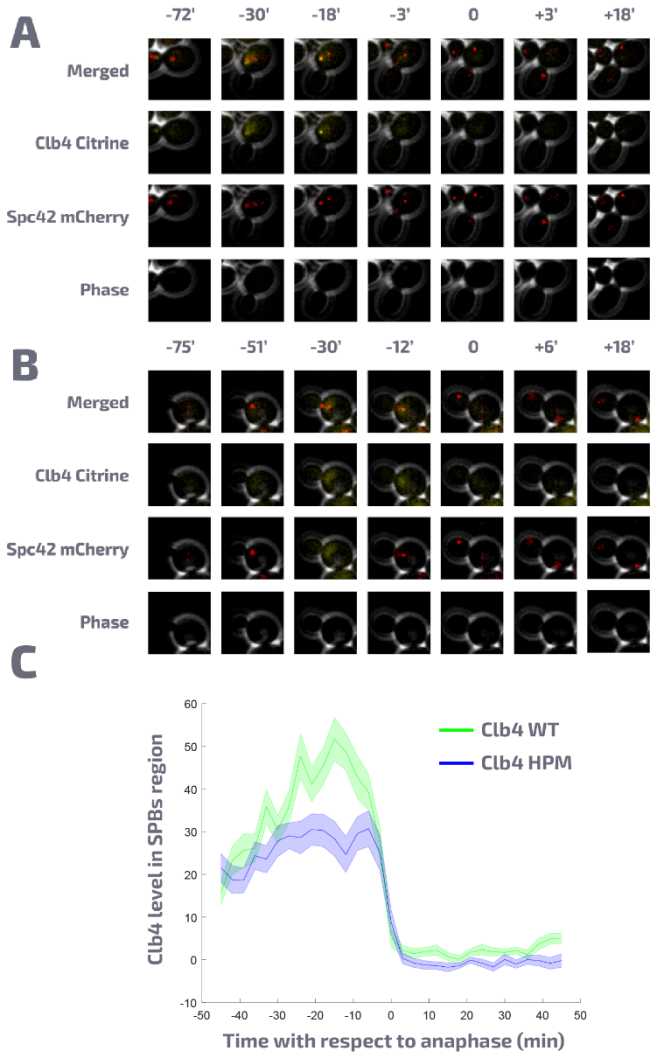

Figure 10. The hydrophobic patch is essential for Clb4 localization. (A, B) Examplary images of cells expressing wild-type Clb4-Citrine (A) and Clb4(HPM)-Citrine (B) together with Spc42-mCherry as a marker for SPB localization. Timepoint 0 corresponds to the onset of anaphase, determined by rapid segregation of Spc42-mCherry-labeled SPBs into two daughter cells. (C) Plot showing the mean±SEM fluorescence levels of Clb4(WT)-Citrine and Clb4(HPM)-Citrine in the SPB region ±45 minutes relative to anaphase entry.

3.2.4 Hydrophobic patch docking specificity of Clb4-Cdk1

To gain an insight into the hydrophobic patch docking specificity of Clb4-Cdk1, we carried out phosphorylation experiments with a set of previously characterized minimal CDK substrates that contain a phosphorylation site and different cyclin docking motifs (**Figure 11A**). We included five cyclin docking motifs in this analysis: two different RxL motifs (VNRILFP and PRKLQF), Clb5/6 docking motif NLxxxL, Clb3 binding motif PxxPxF and mitotic cyclin docking motif LxF. Also, a substrate without any docking motif and histone H1 were

included. The *in vitro* phosphorylation experiments showed that phosphorylation by Clb3-Cdk1 is promoted by the presence of RxL and PxxPxF motifs in the substrate (**Figure 11B**). This is in correlation with published results (Örd *et al.*, 2020). Clb4-Cdk1, however, while having strong activity towards histone H1, phosphorylated all of the minimal substrates with extremely low efficiency (**Figure 11C**). While one of the RxL motifs (VNRILFP) did slightly enhance phosphorylation by Clb4-Cdk1, the docking effect was much weaker than what has been observed with other cyclin-Cdk1 complexes (Örd *et al.*, 2020).

This indicates that Clb4 does not bind strongly to these docking motifs, suggesting that in contrast to all other Clb cyclins, Clb4 does not use RxL motifs in substrate targeting. Also, while the NLxxxL and LxF motifs are used by both S cyclins Clb5/6 and both M cyclins Clb1/2, respectively, this finding suggests that G2 cyclins have diverged in their substrate targeting mechanisms. This is supports previous results that G2 cyclins Clb3 and Clb4 can only compensate for the deletion of the other in some, but not all of their functions (Maekawa & Schiebel, 2004; Örd *et al.*, 2020). Also, this highlights the uniqueness of Clb4 compared to other Clb cyclins. As there are many RxL-containing proteins, the loss of RxL binding could be important for the specialized function and localization of Kar9, as it could strongly decrease substrate competition.

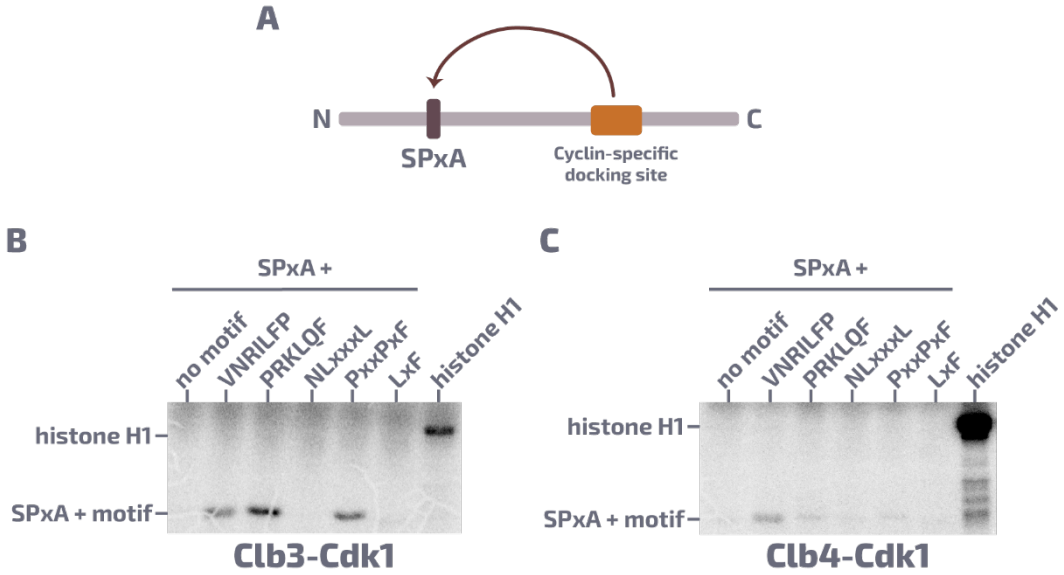

Figure 11. RxL, NLxxxL, PxxPxF and LxF motifs do not strongly promote phosphorylation by Clb4-Cdk1. (A) Scheme of the minimal substrate used in kinase assays presented in panels 'B' and 'C'. The substrate contains a minimal consensus phosphorylation site (SPxA) and a cyclin docking motif. (B, C) Autoradiographs showing the phosphorylation of histone H1 or the substrate proteins with the indicated docking motif by Clb3-Cdk1 (B) or Clb4-Cdk1 (C).

3.2.5 Prediction of potential Clb4-Cdk1 targets

Having identified two instances of similar Clb4/5 binding motifs – VGK**NPF**ASDE from Sic1 and NAI**NPFF**DPE from Kar9, we investigated whether additional NPF-containing potential Clb4-Cdk1 substrate proteins could be predicted. We used an *in silico* tool PSSMSearch to first create a position-specific scoring matrix (PSSM) based on the Sic1 and Kar9 peptides and then searched for peptides with high similarity to the PSSM (Krystkowiak *et al.*, 2018). We limited our search to the intrinsically disordered regions of the *S. cerevisiae* proteome, as most of the linear motifs are in disordered regions. The search revealed in 129 motif hits from 108 proteins (**Appendix Table 1**). Next, as Clb4 is localized to the SPBs, we filtered the hits based on SPB localization, after what five proteins remained. In addition to Kar9, these included Kar1, Stu1, Mlp2 and Cdc11. Interestingly, of these, Kar1, Cdc11 and Mlp1 are physical interactors of Cdk1, while Stu1 has a negative genetic interaction with Clb4 (Costanzo *et al.*, 2016; Sinha *et al.*, 2007; Ubersax *et al.*, 2003; Wong *et al.*, 2007). Interestingly, in Kar1, the predicted NPF motif is located at a similar distance from a CDK consensus phosphorylation site as T548 in Kar9, and further sequence similarities could be observed around the site T149 in Kar1 and T548 in Kar9 (**Figure 12**). The found similarities need to be tested experimentally, but they could offer important insights to the specificity determinants of NPF motifs and the cyclin phospho-docking that has not been described in sufficient detail. Importantly, these predictions indicate that other SPB proteins could be regulated by Clb4-Cdk1 and the NPF motif.

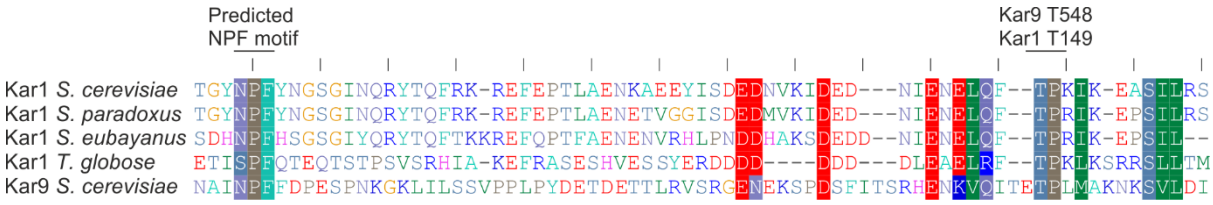

Figure 12. Multiple sequence alignment of predicted NPF motifs in Kar1 and Kar9 and phosphorylation sites T149 and T548 in Kar1 and Kar9, respectively.

SUMMARY

CDKs coordinate the cell cycle by phosphorylating hundreds of substrate proteins in an ordered manner. This is mediated by a complex set of interactions between the substrates and the CDK complex. A key role in this is played by the cyclins. Cyclins are central to CDK substrate targeting, as they can directly bind to substrate proteins via docking motifs. Moreover, cyclins determine the subcellular localization of the CDK complex by guiding CDK to specific subcellular compartments. In this thesis, we investigated the substrate recognition mechanisms of the G2 phase Clb4-Cdk1 complex.

CDK signalling is often mediated by conserved linear motifs that are in intrinsically disordered regions of substrates. Therefore, we started by sequence analysis of Kar9, which led to the identification of a conserved NPFF sequence. This is similar to NPF sequence present in a previously identified S phase cyclin Clb5 docking region in Sic1. To gain a better understanding of these motifs, we verified that NPF is the functional core of the Clb5 docking motif in Sic1 and that the NPFF motif in Kar9 is essential for Kar9 phosphorylation by Clb4-Cdk1 *in vitro*.

Previous studies have only analysed the two full consensus CDK phosphorylation sites in Kar9, but there are also 14 minimal consensus phosphorylation sites. Our *in vitro* phosphorylation experiments indicate that Clb4-Cdk1 multiphosphorylates the C-terminal sites of Kar9. However, we did not observe phosphorylation of full consensus site S197, which is a key target in Kar9 regulation *in vivo*. This indicates that S197 phosphorylation requires either additional factors or significantly higher kinase activity compared to phosphorylation of the C-terminal sites. Analysis of phosphorylation site mutations in Kar9 revealed that a minimal consensus site T548 is a primary target site and that phosphorylation of T548 is necessary for multisite phosphorylation of Kar9. Thus, we identified multiple interactions that drive specific phosphorylation of Kar9 by Clb4-Cdk1.

Next, we investigated the hydrophobic patch docking specificity of Clb4-Cdk1 toward so far identified docking motifs of S/G2/M phase cyclins. We found that these motifs do not considerably promote phosphorylation by Clb4-Cdk1. This analysis included the RxL motif that is conserved in yeast and human genome. It is used by all other S/G2/M phase cyclins, but not by Clb4, indicating that Clb4 has evolved a unique substrate specificity. The loss of docking to RxL motifs could decrease substrate competition for binding to Clb4-Cdk1, as there are many Cdk1 substrates containing RxL docking motifs. Such a unique lack of RxL

docking could explain the apparent low number of substrates of Clb4-Cdk1 and its highly specific function and localization. We found that the cyclin hydrophobic patch is essential in recruiting Clb4 at the microtubule ends. As previous studies have shown that Kar9 anchors Clb4 to the microtubule ends, it allows us to suggest that the hydrophobic patch could be involved in Kar9 binding.

We performed *in silico* analysis to predict NPF motifs. Combining this with Clb4 co-localization data we identified additional potential Clb4-Cdk1 targets. Investigation of these substrate proteins could provide a more detailed understanding of the regulation mediated by Cdk1 in G2 phase. Further experiments are necessary to test these predictions. This work provides the first insights into Clb4-Cdk1 substrate targeting mechanisms that are considerably different compared to other S/G2/M phase cyclins. Also, the presented work illustrates the diversity of interactions that allow Cdk1 to differentially phosphorylate a vast set of substrates.

REFERENCES

Ang, X. L., & Wade Harper, J. (2005). SCF-mediated protein degradation and cell cycle control. *Oncogene*, *24*(17), 2860–2870. https://doi.org/10.1038/sj.onc.1208614

Asfaha, J. B., Örd, M., Carlson, C. R., Faustova, I., Loog, M., & Morgan, D. O. (2022). Multisite phosphorylation by Cdk1 initiates delayed negative feedback to control mitotic transcription. *Current Biology : CB*, *32*(1), 256-263.e4. https://doi.org/10.1016/j.cub.2021.11.001

Bailly, E., Cabantous, S., Sondaz, D., Bernadac, A., & Simon, M. N. (2003). Differential cellular localization among mitotic cyclins from *Saccharomyces cerevisiae*: a new role for the axial budding protein Bud3 in targeting Clb2 to the mother-bud neck. *Journal of Cell Science*, *116*(Pt 20), 4119–4130. https://doi.org/10.1242/JCS.00706

Bállega, E., Carballar, R., Samper, B., Ricco, N., Ribeiro, M. P., Bru, S., Jiménez, J., & Clotet, J. (2019). Comprehensive and quantitative analysis of G1 cyclins. A tool for studying the cell cycle. *PLOS ONE*, *14*(6), e0218531. https://doi.org/10.1371/journal.pone.0218531

Bandyopadhyay, S., Bhaduri, S., Örd, M., Davey, N. E., Loog, M., & Pryciak, P. M. (2020). Comprehensive Analysis of G1 Cyclin Docking Motif Sequences that Control CDK Regulatory Potency In Vivo. *Current Biology : CB*, *30*(22), 4454-4466.e5. https://doi.org/10.1016/J.CUB.2020.08.099

Ben-David, U., & Amon, A. (2020). Context is everything: aneuploidy in cancer. *Nature Reviews Genetics*, *21*(1), 44–62. https://doi.org/10.1038/s41576-019-0171-x

Bhaduri, S., Valk, E., Winters, M. J., Gruessner, B., Loog, M., & Pryciak, P. M. (2015). A docking interface in the cyclin Cln2 promotes multi-site phosphorylation of substrates and timely cell-cycle entry. *Current Biology : CB*, *25*(3), 316–325. https://doi.org/10.1016/j.cub.2014.11.069

Bloom, J., Cristea, I. M., Procko, A. L., Lubkov, V., Chait, B. T., Snyder, M., & Cross, F. R. (2011). Global analysis of Cdc14 phosphatase reveals diverse roles in mitotic processes. *The Journal of Biological Chemistry*, *286*(7), 5434–5445. https://doi.org/10.1074/jbc.M110.205054

Bloom, J., & Cross, F. R. (2007). Multiple levels of cyclin specificity in cell-cycle control. *Nature Reviews Molecular Cell Biology*, *8*(2), 149–160. https://doi.org/10.1038/nrm2105

Chi, Y., Welcker, M., Hizli, A. A., Posakony, J. J., Aebersold, R., & Clurman, B. E. (2008). Identification of CDK2 substrates in human cell lysates. *Genome Biology*, *9*(10), R149. https://doi.org/10.1186/GB-2008-9-10-R149

Costanzo, M., VanderSluis, B., Koch, E. N., Baryshnikova, A., Pons, C., Tan, G., Wang, W., Usaj, M., Hanchard, J., Lee, S. D., Pelechano, V., Styles, E. B., Billmann, M., van Leeuwen, J., van Dyk, N., Lin, Z. Y., Kuzmin, E., Nelson, J., Piotrowski, J. S., … Boone, C. (2016). A global genetic interaction network maps a wiring diagram of cellular function. *Science (New York, N.Y.)*, *353*(6306). https://doi.org/10.1126/SCIENCE.AAF1420

Doncic, A., Eser, U., Atay, O., & Skotheim, J. M. (2013). An algorithm to automate yeast segmentation and tracking. *PloS One*, *8*(3). https://doi.org/10.1371/JOURNAL.PONE.0057970

Enserink, J. M., & Kolodner, R. D. (2010). An overview of Cdk1-controlled targets and processes. *Cell Division*, *5*(1), 11. https://doi.org/10.1186/1747-1028-5-11

Faustova, I., Bulatovic, L., Matiyevskaya, F., Valk, E., Örd, M., & Loog, M. (2021). A new linear cyclin docking motif that mediates exclusively S-phase CDK-specific signaling. *The EMBO Journal*, *40*(2). https://doi.org/10.15252/embj.2020105839

Jackson, L. P., Reed, S. I., & Haase, S. B. (2006). Distinct Mechanisms Control the Stability of the Related S-Phase Cyclins Clb5 and Clb6. *Molecular and Cellular Biology*, *26*(6), 2456–2466. https://doi.org/10.1128/MCB.26.6.2456-2466.2006

Janke, C., Magiera, M. M., Rathfelder, N., Taxis, C., Reber, S., Maekawa, H., Moreno-Borchart, A., Doenges, G., Schwob, E., Schiebel, E., & Knop, M. (2004). A versatile toolbox for PCR-based tagging of yeast genes: new fluorescent proteins, more markers and promoter substitution cassettes. *Yeast*, *21*(11), 947–962. https://doi.org/10.1002/YEA.1142

Jiménez, J., Ricco, N., Grijota-Martínez, C., Fadó, R., & Clotet, J. (2013). Redundancy or specificity? The role of the CDK Pho85 in cell cycle control. *International Journal of Biochemistry and Molecular Biology*, *4*(3), 140–149.

Kao, L., Wang, Y. T., Chen, Y. C., Tseng, S. F., Jhang, J. C., Chen, Y. J., & Teng, S. C. (2014). Global Analysis of Cdc14 Dephosphorylation Sites Reveals Essential Regulatory Role in Mitosis and Cytokinesis. *Molecular & Cellular Proteomics : MCP*, *13*(2), 594. https://doi.org/10.1074/MCP.M113.032680

Kataria, M., Mouilleron, S., Seo, M.-H., Corbi-Verge, C., Kim, P. M., & Uhlmann, F. (2018). A PxL motif promotes timely cell cycle substrate dephosphorylation by the Cdc14 phosphatase. *Nature Structural & Molecular Biology*, *25*(12), 1093–1102. https://doi.org/10.1038/s41594-018-0152-3

Kõivomägi, M., Örd, M., Iofik, A., Valk, E., Venta, R., Faustova, I., Kivi, R., Balog, E. R. M., Rubin, S. M., & Loog, M. (2013). Multisite phosphorylation networks as signal processors for Cdk1. *Nature Structural & Molecular Biology*, *20*(12), 1415–1424. https://doi.org/10.1038/nsmb.2706

Kõivomägi, M., & Skotheim, J. M. (2014). Docking interactions: cell-cycle regulation and beyond. *Current Biology : CB*, *24*(14). https://doi.org/10.1016/J.CUB.2014.05.060

Kõivomägi, M., Valk, E., Venta, R., Iofik, A., Lepiku, M., Morgan, D. O., & Loog, M. (2011). Dynamics of Cdk1 Substrate Specificity during the Cell Cycle. *Molecular Cell*, *42*(5), 610–623. https://doi.org/10.1016/j.molcel.2011.05.016

Krystkowiak, I., Manguy, J., & Davey, N. E. (2018). PSSMSearch: a server for modeling, visualization, proteome-wide discovery and annotation of protein motif specificity determinants. *Nucleic Acids Research*, *46*(W1), W235–W241. https://doi.org/10.1093/NAR/GKY426

Kumar, A., Meier, S. M., Farcas, A.-M., Manatschal, C., Barral, Y., & Steinmetz, M. O. (2021). Structure and regulation of the microtubule plus-end tracking protein Kar9. *Structure*, *29*(11), 1266-1278.e4. https://doi.org/10.1016/j.str.2021.06.012

Kumar, M., Michael, S., Alvarado-Valverde, J., Mészáros, B., Sámano-Sánchez, H., Zeke, A., Dobson, L., Lazar, T., Örd, M., Nagpal, A., Farahi, N., Käser, M., Kraleti, R., Davey, N. E., Pancsa, R., Chemes, L. B., & Gibson, T. J. (2022). The Eukaryotic Linear Motif resource: 2022 release. *Nucleic Acids Research*, *50*(D1), D497–D508. https://doi.org/10.1093/nar/gkab975

Lengefeld, J., Hotz, M., Rollins, M., Baetz, K., & Barral, Y. (2017). Budding yeast Wee1 distinguishes spindle pole bodies to guide their pattern of age-dependent segregation. *Nature Cell Biology*, *19*(8), 941–951. https://doi.org/10.1038/ncb3576

Liakopoulos, D., Kusch, J., Grava, S., Vogel, J., & Barral, Y. (2003). Asymmetric loading of Kar9 onto spindle poles and microtubules ensures proper spindle alignment. *Cell*, *112*(4), 561–574. https://doi.org/10.1016/s0092-8674(03)00119-3

Liu, J., & Kipreos, E. T. (2000). Evolution of Cyclin-Dependent Kinases (CDKs) and CDK-Activating Kinases (CAKs): Differential Conservation of CAKs in Yeast and Metazoa. *Molecular Biology and Evolution*, *17*(7), 1061–1074. https://doi.org/10.1093/oxfordjournals.molbev.a026387

Lu, D., Hsiao, J. Y., Davey, N. E., van Voorhis, V. A., Foster, S. A., Tang, C., & Morgan, D. O. (2014). Multiple mechanisms determine the order of APC/C substrate degradation in mitosis. *Journal of Cell Biology*, *207*(1), 23–39. https://doi.org/10.1083/jcb.201402041

Maekawa, H., & Schiebel, E. (2004). Cdk1-Clb4 controls the interaction of astral microtubule plus ends with subdomains of the daughter cell cortex. *Genes & Development*, *18*(14), 1709–1724. https://doi.org/10.1101/gad.298704

Maekawa, H., Usui, T., Knop, M., & Schiebel, E. (2003). Yeast Cdk1 translocates to the plus end of cytoplasmic microtubules to regulate bud cortex interactions. *The EMBO Journal*, *22*(3), 438–449. https://doi.org/10.1093/emboj/cdg063

Manatschal, C., Farcas, A.-M., Degen, M. S., Bayer, M., Kumar, A., Landgraf, C., Volkmer, R., Barral, Y., & Steinmetz, M. O. (2016). Molecular basis of Kar9-Bim1 complex function during mating and spindle positioning. *Molecular Biology of the Cell*. https://doi.org/10.1091/mbc.E16-07-0552

Matthews, H. K., Bertoli, C., & de Bruin, R. A. M. (2022). Cell cycle control in cancer. *Nature Reviews Molecular Cell Biology*, *23*(1), 74–88. https://doi.org/10.1038/s41580-021-00404-3

McGrath, D. A., Balog, E. R. M., Kõivomägi, M., Lucena, R., Mai, M. v, Hirschi, A., Kellogg, D. R., Loog, M., & Rubin, S. M. (2013). Cks confers specificity to phosphorylation-dependent CDK signaling pathways. *Nature Structural & Molecular Biology*, *20*(12), 1407–1414. https://doi.org/10.1038/nsmb.2707

Moore, J. K., & Miller, R. K. (2007). The cyclin-dependent kinase Cdc28p regulates multiple aspects of Kar9p function in yeast. *Molecular Biology of the Cell*, *18*(4), 1187–1202. https://doi.org/10.1091/mbc.e06-04-0360

Morgan, D. O. (2007). Cell Cycle: Principles of Control. *The Yale Journal of Biology and Medicine*, *80*(3).

Örd, M. (2021). *Ordering the phosphorylation of cyclin-dependent kinase Cdk1 substrates in the cell cycle* [University of Tartu]. http://hdl.handle.net/10062/71673

Örd, M., & Loog, M. (2019). How the cell cycle clock ticks. *Molecular Biology of the Cell*, *30*(2), 169–172. https://doi.org/10.1091/mbc.E18-05-0272

Örd, M., & Loog, M. (2020). Detection of Multisite Phosphorylation of Intrinsically Disordered Proteins Using Phos-tag SDS-PAGE. *Methods in Molecular Biology (Clifton, N.J.)*, *2141*, 779–792. https://doi.org/10.1007/978-1-0716-0524-0_40

Örd, M., Möll, K., Agerova, A., Kivi, R., Faustova, I., Venta, R., Valk, E., & Loog, M. (2019). Multisite phosphorylation code of CDK. *Nature Structural & Molecular Biology*, *26*(7), 649–658. https://doi.org/10.1038/S41594-019-0256-4

Örd, M., Puss, K. K., Kivi, R., Möll, K., Ojala, T., Borovko, I., Faustova, I., Venta, R., Valk, E., Kõivomägi, M., & Loog, M. (2020). Proline-Rich Motifs Control G2-CDK Target Phosphorylation and Priming an Anchoring Protein for Polo Kinase Localization. *Cell Reports*, *31*(11), 107757. https://doi.org/10.1016/j.celrep.2020.107757

Örd, M., Venta, R., Möll, K., Valk, E., & Loog, M. (2019). Cyclin-Specific Docking Mechanisms Reveal the Complexity of M-CDK Function in the Cell Cycle. *Molecular Cell*, *75*(1), 76-89.e3. https://doi.org/10.1016/j.molcel.2019.04.026

Pietro, F., Echard, A., & Morin, X. (2016). Regulation of mitotic spindle orientation: an integrated view. *EMBO Reports*, *17*(8), 1106–1130. https://doi.org/10.15252/embr.201642292

Pirincci Ercan, D., Chrétien, F., Chakravarty, P., Flynn, H. R., Snijders, A. P., & Uhlmann, F. (2021). Budding yeast relies on G_1 cyclin specificity to couple cell cycle progression with morphogenetic development. *Science Advances*, *7*(23). https://doi.org/10.1126/sciadv.abg0007

Schilf, R. (2018). *Sic1 ja CDK kompleksi vaheliste inhibitoorsete seondumismotiivide kaardistamine* [Master's thesis, University of Tartu]. http://hdl.handle.net/10062/61680

Sinha, I., Wang, Y. M., Philp, R., Li, C. R., Yap, W. H., & Wang, Y. (2007). Cyclin-dependent kinases control septin phosphorylation in Candida albicans hyphal development. *Developmental Cell*, *13*(3), 421–432. https://doi.org/10.1016/J.DEVCEL.2007.06.011

Skop, A. R., White, J. G., Adames, N. R., Cooper, J. A., Carminati, J. L., Stearns, T., Morris, N. R., & Vaughan, K. T. (2001). Control of spindle polarity and orientation in *Saccharomyces cerevisiae*. *Trends in Cell Biology*, *11*(4), 160–166. https://doi.org/10.1016/S0962-8924(01)01954-7

Suzuki, K., Sako, K., Akiyama, K., Isoda, M., Senoo, C., Nakajo, N., & Sagata, N. (2015). Identification of non-Ser/Thr-Pro consensus motifs for Cdk1 and their roles in mitotic regulation of C2H2 zinc finger proteins and Ect2. *Scientific Reports*, *5*(1), 7929. https://doi.org/10.1038/srep07929

Swaffer, M. P., Jones, A. W., Flynn, H. R., Snijders, A. P., & Nurse, P. (2016). CDK Substrate Phosphorylation and Ordering the Cell Cycle. *Cell*, *167*(7), 1750-1761.e16. https://doi.org/10.1016/j.cell.2016.11.034

Takeda, D. Y., Wohlschlegel, J. A., & Dutta, A. (2001). A bipartite substrate recognition motif for cyclin-dependent kinases. *The Journal of Biological Chemistry*, *276*(3), 1993–1997. https://doi.org/10.1074/JBC.M005719200

Thompson, J. D., Higgins, D. G., & Gibson, T. J. (1994). CLUSTAL W: improving the sensitivity of progressive multiple sequence alignment through sequence weighting, position-specific gap penalties and weight matrix choice. *Nucleic Acids Research*, *22*(22), 4673. https://doi.org/10.1093/NAR/22.22.4673

Topacio, B. R., Zatulovskiy, E., Cristea, S., Xie, S., Tambo, C. S., Rubin, S. M., Sage, J., Kõivomägi, M., & Skotheim, J. M. (2019). Cyclin D-Cdk4,6 Drives Cell-Cycle Progression via the Retinoblastoma Protein's C-Terminal Helix. *Molecular Cell*, *74*(4), 758-770.e4. https://doi.org/10.1016/J.MOLCEL.2019.03.020

Ubersax, J. A., Woodbury, E. L., Quang, P. N., Paraz, M., Blethrow, J. D., Shah, K., Shokat, K. M., & Morgan, D. O. (2003). Targets of the cyclin-dependent kinase Cdk1. *Nature*, *425*(6960), 859–864. https://doi.org/10.1038/NATURE02062

Uhlmann, F., Bouchoux, C., & López-Avilés, S. (2011). A quantitative model for cyclin-dependent kinase control of the cell cycle: revisited. *Philosophical Transactions of the Royal Society of London. Series B, Biological Sciences*, *366*(1584), 3572–3583. https://doi.org/10.1098/rstb.2011.0082

Umekawa, M., Shiraishi, D., Fuwa, M., Sawaguchi, K., Mashima, Y., Katayama, T., & Karita, S. (2020). Mitotic cyclin Clb4 is required for the intracellular adaptation to glucose starvation in *Saccharomyces cerevisiae*. *FEBS Letters*, *594*(8), 1329–1338. https://doi.org/10.1002/1873-3468.13722

Vodermaier, H. C. (2004). APC/C and SCF: Controlling Each Other and the Cell Cycle. *Current Biology*, *14*(18), R787–R796. https://doi.org/10.1016/j.cub.2004.09.020

Wittenberg, C., & Reed, S. I. (2005). Cell cycle-dependent transcription in yeast: promoters, transcription factors, and transcriptomes. *Oncogene*, *24*(17), 2746–2755. https://doi.org/10.1038/sj.onc.1208606

Wong, J., Nakajima, Y., Westermann, S., Shang, C., Kang, J. S., Goodner, C., Houshmand, P., Fields, S., Chan, C. S. M., Drubin, D., Barnes, G., & Hazbun, T. (2007). A protein interaction map of the mitotic spindle. *Molecular Biology of the Cell*, *18*(10), 3800–3809. https://doi.org/10.1091/MBC.E07-06-0536

Yu, J., Raia, P., Ghent, C. M., Raisch, T., Sadian, Y., Cavadini, S., Sabale, P. M., Barford, D., Raunser, S., Morgan, D. O., & Boland, A. (2021). Structural basis of human separase regulation by securin and CDK1–cyclin B1. *Nature*, *596*(7870), 138–142. https://doi.org/10.1038/s41586-021-03764-0

Appendix

I. Table of predicted NPF motifs from PSSMSearch.

GeneName	Peptide	SeqStart	SeqStop	PWM Pvalue	IUPred
STE3	ESRNPFSTDS	329	338	5.43E-06	0.416
KAR1	TGYNPFYNGS	93	102	1.34E-05	0.61
KEX2	TNENPFSDPI	774	783	9.05E-06	0.557
CHS2	MTRNPFMVEP	1	10	0.00031523	0.815
RED1	QIQNPFVNTS	508	517	0.00033513	0.533
YAK1	PAPNPFQYDS	137	146	0.00021606	0.699
CDC26	DNHNPFYIRE	114	123	7.67E-05	0.814
PRP16	SMVNPFRNPD	262	271	3.26E-06	0.5
SFL1	MMHNPFASKN	492	501	8.36E-05	0.832
NUP1	GGLNPFTSAT	893	902	3.00E-05	0.596
SRM1	PRLNPFLPRD	73	82	0.00067099	0.455
MRPL25	INANPFLPNK	37	46	0.00010532	0.49
PKC1	THTNPFRDMN	751	760	0.00039087	0.628
TSR4	FSSNPFGGAN	174	183	0.00066267	0.444
TSR4	ANANPFGADS	182	191	6.98E-05	0.513
LSB5	TISNPFGDHN	343	352	0.00023054	0.593
BOS1	DSDNPFSTSE	115	124	4.70E-06	0.596
MET4	INANPFDLDE	133	142	1.70E-05	0.473
CDC11	RNTNPFKQSN	325	334	0.00065253	0.764
KRE6	GLTNPFMGSD	50	59	0.00044226	0.864
KRE6	FSSNPFLGEQ	187	196	8.11E-05	0.419
KAR9	NAINPFFDPE	486	495	7.24E-09	0.66
SWI3	IGKNPFNKPN	782	791	7.24E-07	0.64
DNF1	NIPNPFEDFT	143	152	0.00034418	0.453
VPS17	LDNNPFAEPQ	13	22	2.17E-06	0.955
SKN1	VSGNPFLGSE	48	57	6.88E-06	0.726
PTK1	PTSNPFLKNR	545	554	0.00046687	0.541
TPO5	STENPFEENE	581	590	9.77E-06	0.64
EMC3	EVPNPFNDPS	101	110	2.86E-05	0.534
PXL1	KPRNPFSSQR	31	40	7.46E-05	0.774
EDS1	PYINPFISGR	243	252	0.00024212	0.457
TEL1	DPENPFNDKK	606	615	8.43E-05	0.431
BRN1	ALDNPFEDDM	588	597	0.00014477	0.549
STU1	TMINPFKNLE	1034	1043	2.53E-05	0.417
DSF2	NSPNPFNFEK	204	213	0.00013101	0.687
AIM3	DNLNPFERYK	923	932	0.00080164	0.673
SIC1	VGKNPFASDE	214	223	7.24E-09	0.523
YHR097C	TVINPFRVSP	17	26	0.00063661	0.871
YHR097C	NYNNPFLNED	40	49	1.48E-05	0.893
YAP1801	QSYNPFGTDS	334	343	3.84E-05	0.549
YAP1801	IANNPFVSQT	360	369	1.81E-05	0.693

GeneName	Peptide	SeqStart	SeqStop	PWM Pvalue	IUPred
YAP1801	VLNNPFSRPN	477	486	3.15E-05	0.86
YAP1801	IISNPFQNQT	500	509	0.00047447	0.643
YHR177W	PSENPFFHKF	158	167	0.00032717	0.481
AXL2	PLNNPFDDDA	564	573	0.00021244	0.737
DRS2	ASANPFNDNN	1307	1316	6.30E-05	0.597
DRS2	FIENPFADGN	1329	1338	9.92E-05	0.677
MET10	FATNPFGEAK	5	14	8.07E-05	0.404
YER130C	KTTNPFKSGS	305	314	0.00033513	0.526
UTP7	LELNPFETKK	414	423	0.00024936	0.604
MAM1	TSENPFSSSP	257	266	4.85E-05	0.611
SEC9	HVSNPFNSKR	507	516	0.00037096	0.631
MLP2	SFQNPFTASQ	1592	1601	0.00017987	0.632
VHS2	NFTNPFIISR	265	274	0.00038616	0.608
NUP159	LSENPFTSAN	430	439	8.29E-05	0.501
NUP159	SVENPFLPAK	909	918	0.00035359	0.783
YIL092W	AQFNPFMTNE	482	491	1.56E-05	0.531
YIL092W	EVINPFLVNT	617	626	0.00034527	0.514
INP51	RDPNPFVENE	929	938	3.00E-05	0.588
GCD14	AKFNPFGKGS	321	330	0.00094822	0.476
ALY2	RHDNPFFTDL	848	857	6.98E-05	0.54
BBC1	VGFNPFGMAS	435	444	8.29E-05	0.763
BBC1	PSSNPFFRKS	485	494	0.00010025	0.745
PTK2	HTSNPFLKKE	606	615	2.97E-05	0.674
IBA57	PTLNPFTNKP	414	423	0.0004191	0.766
CTH1	PINNPFAGNN	113	122	0.00048605	0.583
TIS11	QLMNPFLPSA	87	96	0.00076653	0.492
DSK2	TAANPFASLL	274	283	8.83E-05	0.563
DSK2	PALNPFANAG	285	294	6.44E-05	0.533
NUP42	SGINPFTNNA	20	29	2.90E-06	0.646
NUP42	ATSNPFGKSP	129	138	0.00067859	0.584
CCH1	PNTNPFGDNA	14	23	0.00015164	0.812
PSP2	SKSNPFGSAK	236	245	0.00012812	0.598
AVT4	LNSNPFYSRK	37	46	5.65E-05	0.525
ROM2	ITSNPFSDPH	320	329	7.24E-07	0.884
YIP5	NEPNPFDDAT	23	32	0.00010423	0.835
PRP43	GKINPFTGRE	69	78	3.15E-05	0.503
YGL082W	YISNPFSDQN	281	290	0.0002157	0.682
CDH1	TNLNPFMNNT	3	12	8.07E-05	0.761
SLX9	FQKNPFGALR	193	202	0.00054685	0.436
YAP1802	DAYNPFGSQQ	337	346	1.01E-05	0.744
YAP1802	PTANPFLIPQ	370	379	7.24E-05	0.793
YAP1802	GSNNPFSLEN	450	459	0.00054432	0.823
YAP1802	NSPNPFTLQQ	471	480	8.11E-05	0.772
FPK1	SSNNPFRERA	233	242	0.00051681	0.73
TDA7	SANNPFSNEF	532	541	9.30E-05	0.651
YNL058C	LQSNPFDIND	146	155	0.00098585	0.512

GeneName	Peptide	SeqStart	SeqStop	PWM Pvalue	IUPred
SUR7	SRWNPFHREK	231	240	0.00084398	0.502
SLG1	TDINPFDDSR	341	350	4.09E-05	0.642
RHO4	TIKNPFKRNT	252	261	0.00030184	0.62
SED5	NNSNPFMTSL	203	212	0.00015164	0.64
MLP1	GGFNPFTSPS	1724	1733	1.81E-06	0.844
RSN1	KENNPFADPK	934	943	7.24E-07	0.701
OYE2	RVTNPFLTEG	292	301	0.000477	0.401
TAF8	RTKNPFLKIS	300	309	0.00029786	0.43
YDR239C	KNTNPFLNAE	85	94	1.63E-05	0.704
YDR239C	QRTNPFTTSA	128	137	0.00056821	0.751
SNX41	EDNNPFVGTH	24	33	0.00093519	0.678
SIZ1	LIVNPFIPRR	858	867	0.00065905	0.534
DLT1	YSINPFDENE	265	274	2.90E-06	0.438
SPO20	KSPNPFRKKR	252	261	0.00069343	0.592
GFD1	LAINPFSQKA	93	102	2.32E-05	0.712
PAL1	SVNNPFRNAT	14	23	0.00080635	0.643
PAL1	SSKNPFLDDV	103	112	1.45E-06	0.73
ENT2	GSNNPFSMDN	344	353	0.00010821	0.912
ENT2	PKNNPFLSNQ	488	497	8.11E-05	0.8
YLR352W	SSANPFAINV	641	650	0.00034382	0.606
ATG20	EKDNPFMEEG	74	83	0.00054541	0.7
HBT1	FSSNPFDDSK	767	776	8.98E-05	0.762
ISA1	NNVNPFKLKF	37	46	0.00066158	0.448
YEH2	AAENPFQNIA	130	139	0.00031342	0.436
CSI2	DSTNPFNYTS	292	301	0.00078354	0.511
HRK1	LSRNPFHGHH	5	14	0.00026203	0.904
OXR1	DSHNPFRNKT	38	47	0.00035359	0.696
TRM8	AHSNPFSDHQ	57	66	5.90E-05	0.529
YLR053C	KKHNPFYVPS	83	92	6.66E-05	0.498
YPR022C	PPQNPFGDPL	318	327	5.10E-05	0.902
PSH1	ASTNPFANRD	211	220	1.85E-05	0.68
YOR342C	QRQNPFCSTE	302	311	1.56E-05	0.612
LCB4	ISSNPFQTEN	97	106	6.98E-05	0.626
PHM7	TPSNPFESGS	764	773	0.00036409	0.847
TAF3	IQENPFVTSK	247	256	6.88E-05	0.573
LAS17	SATNPFPFPV	284	293	0.00011907	0.926
SFG1	EITNPFMTEG	79	88	0.00070284	0.437
ENT1	MSNNPFAKSE	303	312	2.53E-06	0.848
ENT1	PNHNPFLNSQ	404	413	0.000211	0.774
Q0297	GGPNPFLRRS	33	42	0.00028772	0.655

NON-EXCLUSIVE LICENCE TO REPRODUCE THESIS AND MAKE THESIS PUBLIC

I, Dmytro Fedorenko,

1. grant the University of Tartu a free permit (non-exclusive licence) to: reproduce, for the purpose of preservation, including for adding to the DSpace digital archives until the expiry of the term of copyright, my thesis

"The substrate targeting mechanisms of Clb4-Cdk1", supervised by Ilona Faustova, Mihkel Örd.

2. I grant the University of Tartu the permit to make the thesis specified in point 1 available to the public via the web environment of the University of Tartu, including via the DSpace digital archives, under the Creative Commons licence CC BY NC ND 4.0, which allows, by giving appropriate credit to the author, to reproduce, distribute the work and communicate it to the public, and prohibits the creation of derivative works and any commercial use of the work from ***27/05/2025*** until the expiry of the term of copyright.

3. I am aware of the fact that the author retains the rights specified in p. 1 and 2.

4. I certify that granting the non-exclusive licence does not infringe other persons' intellectual property rights or rights arising from the personal data protection legislation.

Dmytro Fedorenko

27/05/2022